AUTOMATIC CONTROL OF AN INERTIAL ELECTROSTATIC CONFINEMENT DEVICE

By

Micah K. Condie

A thesis submitted in partial fulfillment of the requirements for the degree of

Bachelor of Science

Houghton College

May 2023

Signature of Author……..
Department of Physics
May 10, 2023

……
Dr. Mark Yuly
Professor of Physics
Research Supervisor

……
Dr. Katrina Koehler
Assistant Professor of Physics

AUTOMATIC CONTROL OF AN INERTIAL ELECTROSTATIC CONFINEMENT DEVICE

By

Micah K. Condie

Submitted to the Department of Physics
on May 10, 2023 in partial fulfillment of the
requirement for the degree of
Bachelor of Science

Abstract

The Houghton University Farnsworth-Hirsch fusor is an inertial electrostatic confinement device designed for the purpose of studying plasmas, D-D fusion, and as a source of x-rays and neutrons for other experiments. It operates via two concentrically arranged wire spheres with a voltage difference between them of up to 30 kV, ionizing a low-pressure gas to form and confine a plasma. The voltage across the two spheres is measured using a voltage divider circuit allowing an Arduino at the bottom of the chain to measure a lower proportional voltage. The current from the HV grid to the power supply flows through an LED, floating at high voltage, the light from which is then measured at the end of a fiber-optic cable using a phototransistor circuit. The previous fusor remote operating system used LabVIEW and Digi TS4 Port servers to communicate with the high voltage power supply, pressure gauge, and mass-flow controller via ethernet, RS-232, and RS-485. It was redesigned using a python code running on a remote computer to communicate with the instrumentation directly over USB and RS-485. Furthermore, the python code implemented a PID controller so that the pressure in the chamber could be adjusted automatically, maintaining the plasma while raising the voltage. The fusor was tested using air as the ionized gas with limited success using the PID controller. Future experiments will correct the automatic system and test the system with hydrogen then deuterium.

Thesis Supervisor: Dr. Mark Yuly
Title: Professor of Physics

TABLE OF CONTENTS

TABLE OF FIGURES

Chapter 1

OVERVIEW OF INERTIAL ELECTROSTATIC CONFINEMENT FUSION

1.1. The Nature of Inertial Electrostatic Confinement Fusion

Sir Arthur Eddington proposed in 1920 that the seemingly inexhaustible source of energy that comes from the sun is none other than the relativistic energy associated with matter [1]. The process by which matter is converted to energy in this way was later shown to be nuclear fusion. Since the end of World War II, fusion research has been a key area of interest as humans seek to harness the same source of energy as the sun. While uncontrolled fusion, such as that occurring in stars as well as the hydrogen bomb, releases significant amounts of energy, controlling fusion reactions such that the energy can be used for other purposes has proved more difficult. One device for producing controlled fusion reactions is the "Farnsworth fusor", which uses Inertial Electrostatic Confinement (IEC) to generate nuclear fusion reactions. This device works by confining a state of matter known as plasma, using a static electric field.

1.1.1. Plasma

The most abundant form of matter in the universe is plasma, a state consisting of a significant proportion of unbound negatively charged electrons and positively charged ions. Plasma is created when electrons are torn away from the neutral atoms in a gas. If the plasma has a high temperature, the electrons can escape due to the thermal energy in collisions. Confining a high temperature plasma is difficult because the large kinetic energy of the ions and electrons prevents confining the plasma within a physical container. This is because the energy of the ions would be immediately lost to collisions with the walls.

There are four typically used methods for confining a plasma. The first method is what is observed naturally in stars. In this case, gravity confines the plasma (gravitational confinement). Another method is to confine the plasma using a magnetic field (magnetic confinement). The third way is to create and confine a plasma for a very brief period by hitting a small target capsule with high power lasers. The outer shell of the capsule heats up

very quickly, causing it to accelerate outward which compresses the material within the capsule (inertial confinement). The final approach is to use an electrostatic field to confine the plasma. As mentioned before, this method is known as Inertial Electrostatic Confinement (IEC).

While the first two methods for artificially confining a plasma have received significant attention and funding, IEC has been less prominent as an active field of research. Early on this was, in part, due to Earnshaw's theorem, which showed that a static electric field cannot confine a plasma [2]. Since Earnshaw's analysis described a steady-state system, however, it failed to account for the dynamic nature of IEC devices. This early skepticism of IEC methods has continued, however, as funding organizations such as the Department of Energy continue to make major investments in inertial and magnetic confinement research, while IEC research is limited to small scale studies [3]. This is because inertial and magnetic confinement methods are believed to be more likely to be used in a future fusion power source. One benefit of IEC devices is that they are much easier to construct than any other plasma confinement device. For this reason, they are often used to study plasmas, as well as generate fusion reactions in small labs [3].

1.1.2. Fusion

To understand how fusion works, consider the nucleus of an atom. Every nucleus consists of protons and neutrons. The mass of the nucleus they make up is less than the sum of the masses of the constituent nucleons. This difference in mass (Δm) has an energy (E) associated with it according to Einstein's famous equation,

$$E = \Delta m c^2, \tag{1}$$

where c is the speed of light in a vacuum. The energy associated with the difference in mass between the nucleus and its unbound constituents is then,

$$E_b = \left[Z m_p + N m_n - M\left({}^{Z+N}_{Z}X\right)\right]c^2, \tag{2}$$

where Z and N are the number of protons and neutrons in the nucleus X, respectively; $M({}^{Z+N}_{Z}X)$ is the mass of that nucleus; and m_p and m_n are the rest masses of an unbound proton and neutron, respectively. The energy associated with the difference in mass, E_b, is referred to as the binding energy and it is the energy required to break a nucleus into its individual nucleons. Alternatively, it can be understood as the energy released when the nucleons are brought together to form the nucleus. Figure 1 shows the binding energy per nucleon, E_b/A as a function of mass number, $A = N + Z$. It can be observed that for elements with less atomic mass than ^{56}Fe, the lighter nuclei generally have less binding energy per nucleon associated with them than the larger nuclei. This would suggest that if these light nuclei were combined to form larger nuclei, there would be a net release of energy. In fact, this is exactly what happens, and the process of two light nuclei combining to form a larger nucleus is known as nuclear fusion.

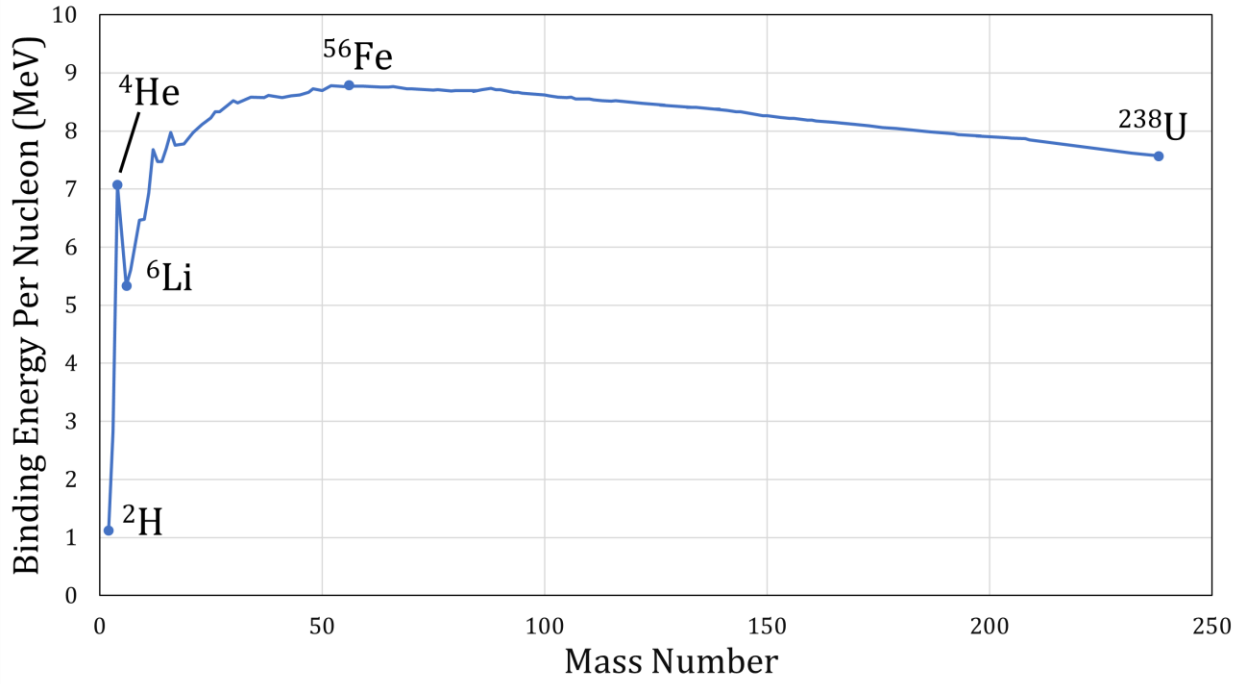

Figure 1. Binding energy per nucleon vs. mass number plot. The binding energy per nucleon generally increases with mass number until ^{56}Fe at which point it begins to drop. This is why energy is released via fusion for lighter nuclei and via fission for heavier nuclei. Data for figure is taken from Ref [4].

The strong nuclear force that holds the nucleus together only acts when nuclei are within approximately one femtometer of each other. The magnitude of the strong nuclear force is much greater than that of the other fundamental forces such as gravity or electromagnetism. Then for fusion to occur, one would expect the nuclei must be within about one femtometer of each other. This is difficult to achieve since all nuclei are positively charged, meaning they will experience Coulomb repulsion. This electromagnetic repelling force, **F**, will increase in intensity as two nuclei come closer together according to Coulomb's law,

$$\mathbf{F} = \frac{e^2}{4\pi\varepsilon_0}\frac{Z_1 Z_2}{r^2}\hat{\mathbf{r}} \tag{3}$$

where Z_1 and Z_2 are the number of protons in each of the nuclei and e is the elementary charge of a proton. Here, ε_0 is the permittivity of free space, r is the distance between the nuclei, and $\hat{\mathbf{r}}$ is the unit vector pointing in the direction opposite the other nucleus. Notice, that at the distance the strong nuclear force will begin to act, r will be slightly more than the sum of the radii of the two nuclei (see Figure 2).

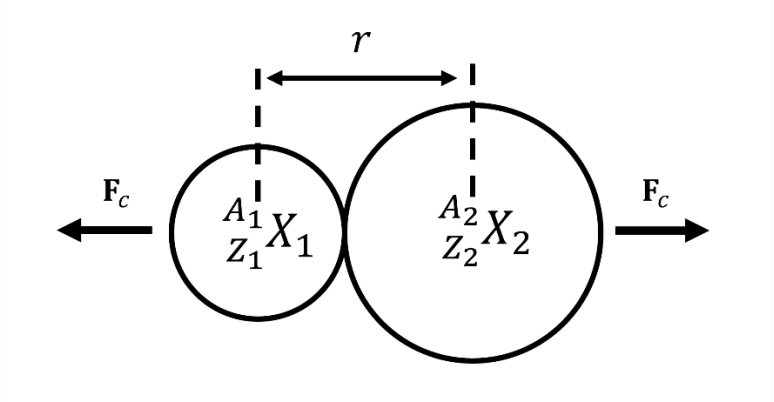

Figure 2. Coulomb repulsion diagram. The two nuclei, X_1 and X_2, experience a coulomb repelling force, $\mathbf{F}_c$ proportional to their proton numbers, Z_1 and Z_2. The force is inversely proportional to the square of the distance between the nuclei, r.

The potential energy associated with the coulomb force can be obtained by integrating the force over the distance of separation. Accordingly,

$$U_c = \frac{e^2}{4\pi\varepsilon_0}\frac{Z_1 Z_2}{r} \tag{4}$$

where r is the distance between the two nuclei and U_c is the potential energy associated with the coulomb force at this state. Furthermore, U_c is defined to be zero at $r = \infty$. This potential energy, U_c, is known as the Coulomb barrier as it is the potential barrier that must be overcome for fusion to occur. The situation can be approximately described by the potential energy plot in Figure 3 which shows the coulomb potential, and the strong force potential approximated by a square well. The total potential energy, $U = U_s + U_c$ is positive until the nuclei are separated by a distance A, approximately one femtometer. At this point the strong nuclear force acts, and brings the potential energy of the system to the stable equilibrium of point B. Notice the potential energy at point B is the binding energy of the new nucleus that has been created by the two nuclei.

Classically, the two nuclei would need to have more kinetic energy than the Coulomb barrier to fuse. For thermonuclear fusion, this would require enormous temperatures. For example, the sun would not be nearly hot enough for fusion to occur. Quantum mechanically, this is not the case, because of the wave nature of matter a particle possesses some probability of penetrating a potential barrier, despite having insufficient kinetic energy to do so classically. This is known as quantum tunneling and the probability of it happening for a rectangular barrier is proportional to

$$T \propto e^{\frac{-2L}{\hbar}\sqrt{2m(U-E)}}, \tag{5}$$

where T is known as the transmission coefficient. Here, m is the mass of the particle, L is the width of the barrier, and U is the height of the energy barrier. As always, $\hbar$ is Planck's constant and E is the kinetic energy of the particle.

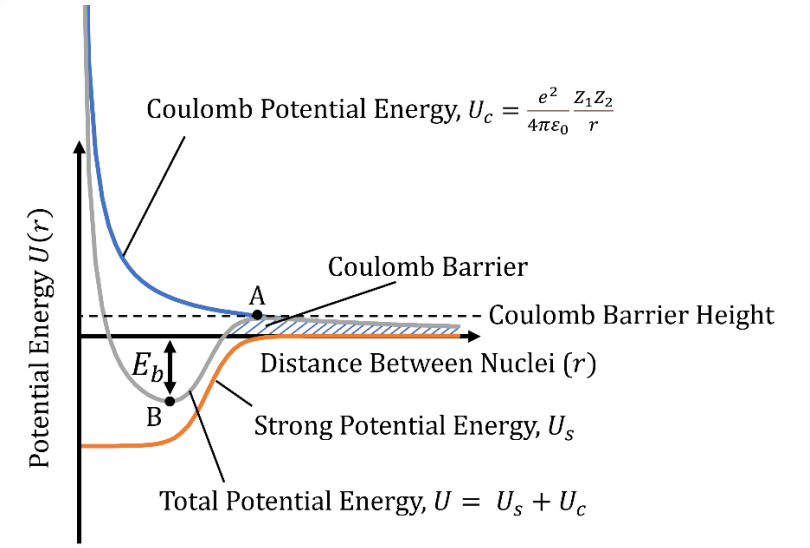

Figure 3. Potential energy as a function of nuclei separation. Point A represents the distance between nuclei where the strong nuclear force begins to act, ultimately bringing the system to stable equilibrium at point B. The strong potential is modeled as a roughly rectangular potential well. The binding energy of the newly created nucleus is E_b. The shaded region is known as the Coulomb barrier, which is the potential barrier that must be overcome for the nuclei to fuse.

As can be seen in Equation (5), the probability of the particle passing through a potential barrier decreases with the width and height of the barrier and increases with the kinetic energy of the particle. This indicates more reactions will occur when the particles have large kinetic energies, such as the highly energetic ions in a plasma. Devices, such as the one Farnsworth created, were designed for this purpose of producing fusion reactions.

1.1.3. Farnsworth Fusor and Gridded IEC Devices

In 1966, the inventor of the television, Philo T. Farnsworth, was awarded a patent for an "Electric Discharge Device for producing interactions between nuclei" [5]. The device, later known as a Farnsworth-Hirsch fusor, became the first of many gridded IEC devices often referred to as simply "fusors". Farnsworth's idea, which was based on his work with the vacuum tubes found in early televisions, was to confine a plasma using an electrostatic field. The purpose of confining the plasma was to produce fusion reactions. Interestingly, a Soviet scientist by the name of Lavrent'ev may have had first the idea of electrostatic confinement of a plasma [6], having suggested it in the early 1950s, around the same time as Farnsworth.

Regardless, Farnsworth's patent described a device that consisted of a penetrable anode made of a wire grid, arranged within a cathode. The wire grid is what gives gridded IEC devices their name.

To understand how gridded IEC devices work, consider a spherical wire mesh suspended within a vacuum chamber. After a low-pressure gas is released into the chamber, the voltage on the wire mesh is raised to the kV range. If the voltage is positive relative to the grounded chamber, a plasma will be created with electrons being accelerated toward the positively charged anode, which is the wire sphere. This is known as an electron injected device and is the type described in Farnsworth's original patent. If the suspended wire sphere is instead negatively charged, as shown in Figure 4, the positively charged ions will be accelerated toward the center. This is an ion-injected device.

Consider what happens as ions approach the cathode in the ion injected configuration of a gridded IEC device. The ions will accelerate until they reach the cathode. At this point, they will have significant kinetic energy, but no potential energy. The ions will then pass through the wire mesh and travel until they reach the other side of the chamber, at which point they will turn around and repeat the process of coming back through the cathode. The electric potential for this configuration is shown in Figure 4a. Because all ions will be attracted to the cathode, there will be a higher density of ions at the center of the spherical mesh due to three dimensional focusing. If there are enough ions, this creates a positively charged region within the wire grid resulting in an increased electric potential at the center of the device as shown in Figure 4b. Farnsworth termed this virtual potential well a poissor. As the number of ions increases, which is related to the current supplied by the power supply, there may be enough electrons accelerating toward the virtual anode, just as the ions accelerated toward the physical cathode, that they too will form a virtual potential well within the virtual anode. The electric potential for the configuration with this virtual cathode can be seen in Figure 4c. In theory, this process could repeat giving any number of onion-skin-like potential wells at the center of the device, but practically it usually ends after the potential well formed by the electrons is created due to angular momentum effects.

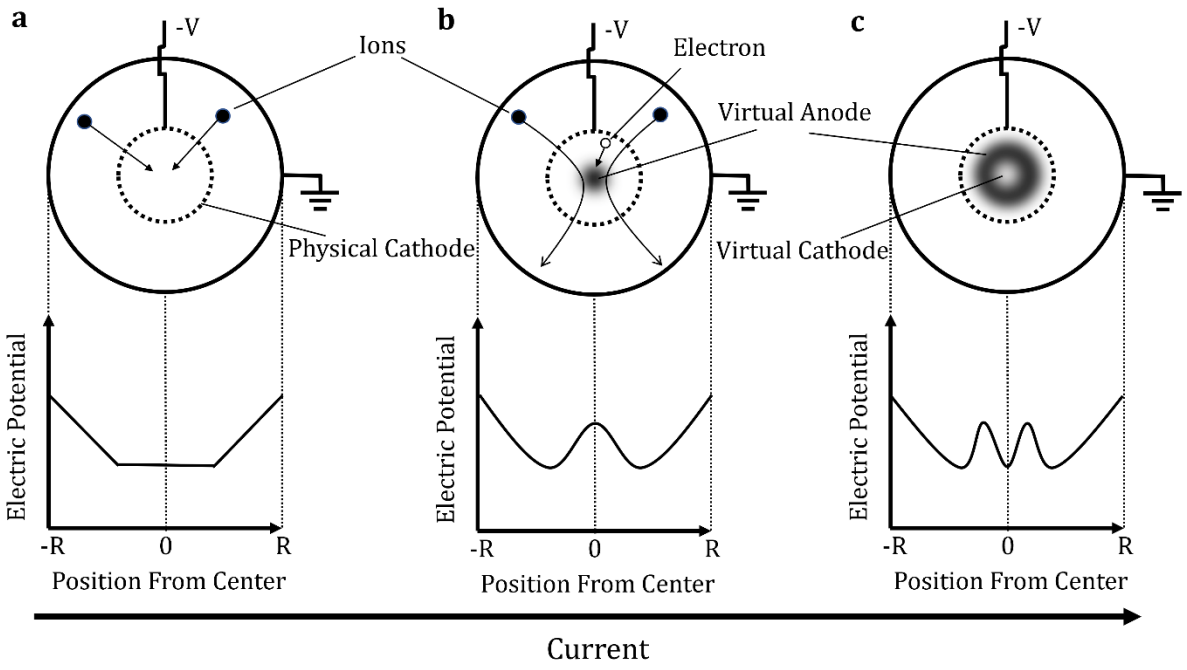

Figure 4. Gridded IEC device and electric potential diagrams as a function of current. In (a) ions are accelerated toward the negatively charged cathode where they have zero potential energy. Due to three dimensional focusing there will be an increased density of ions at the center of the device as can be seen in (b). Electrons will be accelerated toward this positively charged virtual anode, and given sufficient current, these electrons will form a virtual cathode as can be seen in (c).

1.2. Difficulties and Further Development of IEC Devices

As mentioned before, the primary factor driving fusion research is the possibility that it could one day be used as a power source. Current power sources suffer from either low energy density, harmful biproducts, or both. For example, gasoline produces 46 MJ/kg [7] when burned, which is more than almost any chemical reaction, and contributes to air pollution. Nuclear fission is a process similar to fusion except large nuclei are split instead of smaller ones fusing together. The energy density of enriched uranium, which is the commonly used fuel for fission, is much larger than gasoline at 3.9×10^6 MJ/kg [7]. Fission produces radioactive biproducts that are difficult to dispose of, however. Furthermore, the chain reaction responsible for fission leaves open the possibility of thermal runaway, which is a safety concern.

Simply looking at the binding energies, fusion using deuterium and tritium as the fuel would have an energy density over 100 times greater than that of enriched uranium [4]. The products of a D-T reaction are helium and a neutron, neither of which will have to be disposed of as radioactive waste. Furthermore, the possibility of a runaway reaction is nonexistent. For these reasons using controlled fusion as a nuclear reactor would be significantly better than currently used power sources. The difficulty with using thermonuclear fusion as a power source is that a large amount of energy must initially be put into the system to raise the temperature for the nuclei to overcome the Coulomb repulsion. Once enough of the fuel reacts, the energy produced by the reactions will further heat the fuel, meaning external energy no longer needs to be introduced. This point where the process becomes self-sustaining is called ignition. Up until 2022, the only manmade reactions for which ignition occurred were in uncontrolled fusion reactions, such as in the hydrogen bomb. Recent experiments at the National Ignition Facility have reached ignition using ICF [8]. It is still unclear whether the requirements for ignition can be met using other confinement methods, such as IEC.

1.2.1. Requirements for Fusion as a Power Source

In thermonuclear reactions, where there are many ions going in various directions, the average kinetic energy of the individual ions increases with the overall temperature of the plasma. It is intuitive then that a sufficiently high temperature of the plasma is required for ignition to be reached because of the large kinetic energies required for the ions to overcome coulomb repulsion. The temperature where ignition is reached is called the critical ignition temperature. Lawson [9] demonstrated that besides the temperature requirement for fusion, there are two other parameters that affect whether a fusion device will achieve ignition. These are ion density, n, and confinement time, τ. The first parameter, ion density, is intuitive since more ions in a given volume will lead to more reactions occurring. Confinement time is defined as the duration for which the energy put into the plasma stays within it. The longer the ions have a given energy, the more chances they will have to react, increasing the total energy released. The product of ion density and confinement time, $n\tau$, is known as the Lawson number and must be sufficiently large for ignition to occur. For

example, Lawson calculated that for a D-D reaction $n\tau > 10^{16}$ s/cm^3 is required for net power fusion.

When applied to the specific case of electrostatic confinement devices, Lawson's criteria must be altered slightly. Since the ions in IEC devices do not follow a Maxwellian distribution, the temperature criteria for ignition must be understood as the average kinetic energy of the recirculating ions. Since most ions are created near the outer grid, by the time the ions reach the center they will possess kinetic energy equivalent to the product of the ion charge multiplied by the potential difference across the grids. For this reason, fusors seem to easily meet the temperature criterion, since a potential difference of just 15 kV is enough to reach ignition and this is well below the operating voltage of most fusors. Lawson, however, assumed that the electrons and ions were in thermal equilibrium. This is not the case for IEC devices and because electron energy loss processes are common, an additional requirement for the ratio of the electron "temperatures", T_e, and ion "temperatures", T_i, must be observed [3]. As an example, for D-T fusion a ratio of $T_e/T_i < 1/3$ must be maintained. This makes meeting the temperature requirement for ignition more difficult, but still achievable.

As for the Lawson number, theoretically, the ion density at the center potential well of a gridded device should be 10^{16} cm^{-3}, which is 100 times the density achieved by most magnetic confinement devices. This leaves the confinement time as the central issue preventing IEC devices from reaching ignition. Since the confinement time is the amount of time energy put into the system stays in it, for the IEC case it can be understood as the duration a particle spends inside the potential well at each pass, multiplied by the number of recirculations. It becomes clear then that ignition would be achieved if the particles continued to recirculate until they fused. Instead, most particles lose energy due to reactions with either the background gas or with the grid structure. A background neutral gas is required to create the plasma and the fusion between neutral atoms and ions occurs more often than ion-ion fusion. Furthermore, charge exchange reactions are frequent, which result in a high energy neutral atom and a low energy ion. The final way the ions lose energy, causing them to stop recirculating through the core of the device, is through fusion with absorbed gas on the wire grid.

Collisions with the wire grid can be minimized by making the wire grid openings sufficiently large such that ion beams pass through the openings. This is known as "Star" mode and is one of three possible modes in which a fusor can operate [3]. The other two are the "Central Spot" mode and "Halo" mode, the latter of which is produced when a grid opening is larger in a particular location. A diagram of all modes can be seen in Figure 5. Regardless of what mode a fusor is being operated in, any future attempts at using IEC as a power source must either make grids more transparent or eliminate the need for a physical grid altogether. The latter could be achieved by using a magnetic field to electrostatically confine ions as proposed by R.W. Bussard [10]. A further modification required for a fusor to achieve ignition is the ions would need to be introduced from an external source, removing the background neutral gas.

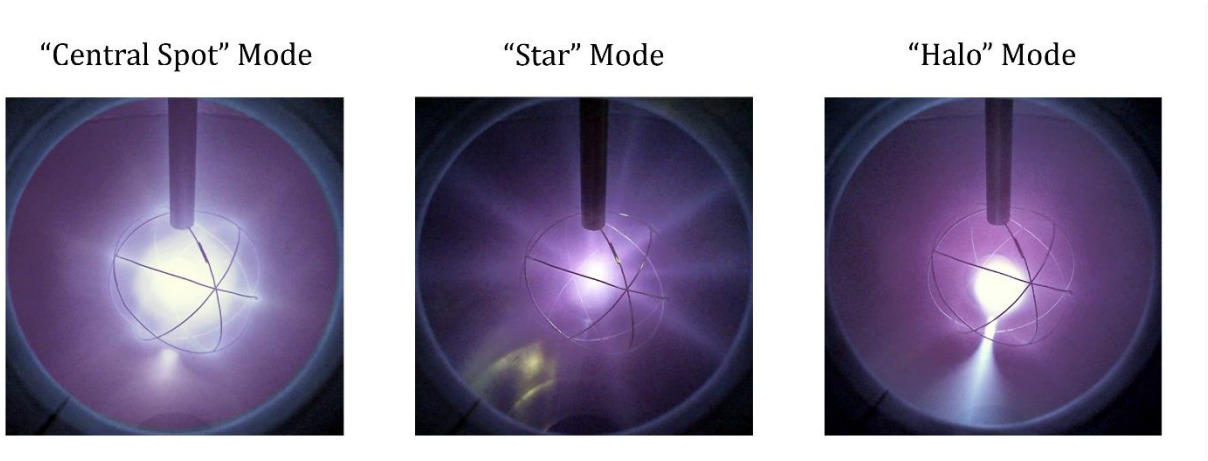

Figure 5. Fusor operating modes. The "Central Spot" mode on the left is the result of evenly distributed and smaller grid openings. The "Star" mode happens when the grid openings are large, and the "Halo" mode is observed when one grid opening is larger than the others. Images from Ref [11].

1.2.2. History of IEC Research

Even before Farnsworth received his patent, Elmore, Tuck, and Watson worked out the theoretical possibility of confining a plasma by projecting electrons radially inward [12]. This possibility was confirmed by Hirsch who worked with Farnsworth, to experimentally demonstrate that both ion and electron injection can be used to confine a plasma [13, 14].

Even in these early experiments, Hirsch used an external ion source as opposed to creating the plasma within the device, seeking to eliminate the background neutral atoms. In an attempt to eliminate the other source of premature ion collisions, Bussard came up with a hybrid IEC magnetic approach that did not rely on a physical cathode [10]. In 1998, research at the Los Alamos National Laboratory resulted in an alternative approach for IEC devices developed by D. C. Barnes and R.A. Nebel which relied on spherical plasma oscillations [15]. George H. Miley helped to popularize IEC devices for reasons other than fusion. Speaking at a conference at the University of Wisconsin, Miley inspired an audience member to create a commercial version of the fusor for neutron activation analysis [16]. Research continues at the University of Wisconsin-Madison and Kyoto University, but little progress has been made since then, as funding continues to go toward other confinement methods [3]. IEC is now used almost exclusively as a neutron source that operates several orders of magnitude below breakeven, where more power is produced by the system than put into the system.

1.3. The Houghton University Fusor

The Houghton Fusor is an ion-injected IEC device created with the intent of eventually studying D-D fusion. It is believed the device will also be useful for studying plasmas as well as using the device as an x-ray and neutron source for other experiments.

1.3.1. Description of the Houghton University Fusor

The device consists of two wire grids arranged concentrically within a vacuum chamber, evacuated with a diffusion pump backed by a rotary fore pump. The outer wire grid is grounded, while the inner one is held at a negative voltage in the kV range using a high voltage power supply. Figure 6 shows a simplified diagram of the device. The pumps evacuate the chamber at a constant rate and a mass flow controller introduces gas into the chamber at a set rate. By controlling the rate at which gas is let into the chamber, the pressure can be adjusted. The low pressures in the chamber and the large potential difference across the electrodes cause a plasma to form.

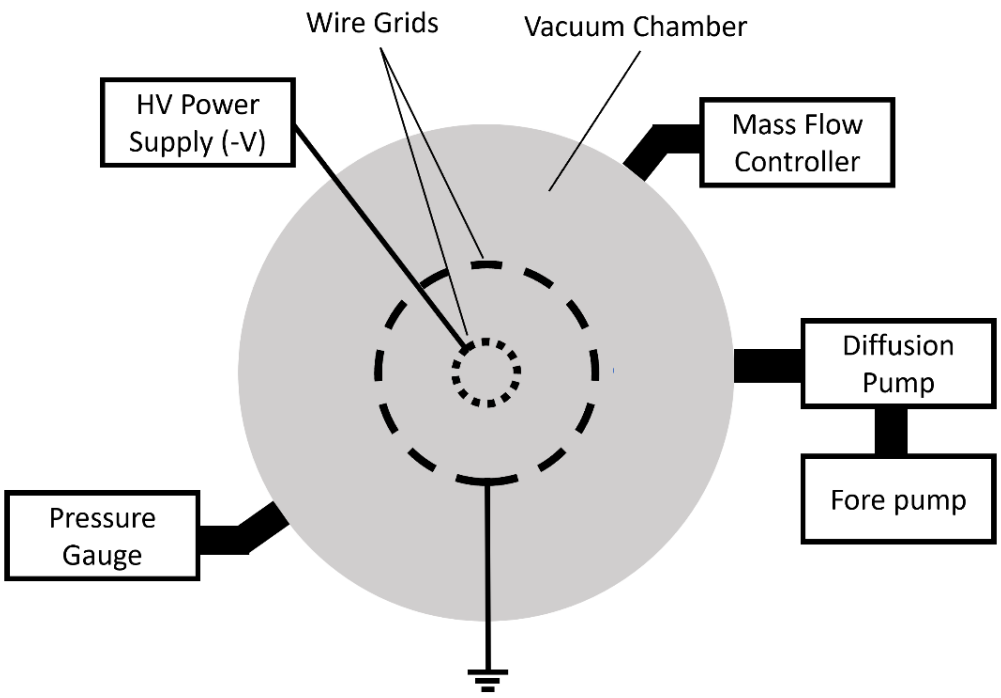

Figure 6. Simplified diagram of the Houghton University Fusor. The fusor consists of a spherical cathode grid within a spherical anode grid both contained in a vacuum chamber. The pressure in the chamber is measured with a pressure gauge and is controlled with a pump system and a mass flow controller.

1.3.2. Previous Work

Construction on the fusor began in 2011 [17]. Within a few years, the device was operational such that an air plasma could be created and confined. A radiation survey meter was used to measure the intensity of the bremsstrahlung X-rays as a function of distance from a thin Mylar (BoPET) foil window. A CdTe detector was used to measure the energy spectrum of the x-rays. Since the next step was to use the device to create neutron producing D-D reactions, a system was created so the fusor could be controlled remotely [18]. This way, future experiments with deuterium could be done safely from a distance. The remote control system used a LabView interface which communicated over an ethernet network with the pressure gauge, mass flow controller, and high voltage power supply using two Digi TS4 Port servers via RS232 and RS485 serial interfaces. After mandatory upgrades of both Windows 10 and LabView, however, communication with the instruments was no longer supported.

Issues developed with the fusor itself as well. There was sparking within the chamber near the HV feed through system when the system was filled with hydrogen gas. Ceramic beads were added to the HV wire between the chamber wall and the rod going to the cathode as shown on the left of Figure 7, but this failed to solve the issue. Two nylon cylinders as shown on the right of Figure 7 were then added to keep the HV wire centered as it enters the chamber, keeping it as far away as possible from the grounded walls. This solution was never tested since the current meter on the high voltage power supply broke, meaning there was no way to measure current. Efforts were made to remedy the remote system problems by directly communicating with the instrumentation through LabVIEW, getting rid of the Digi port server design, and using a National Instruments I/O device to control the power supply. This configuration was never used since the LabView license expired and the lab switched to python as its main programming language.

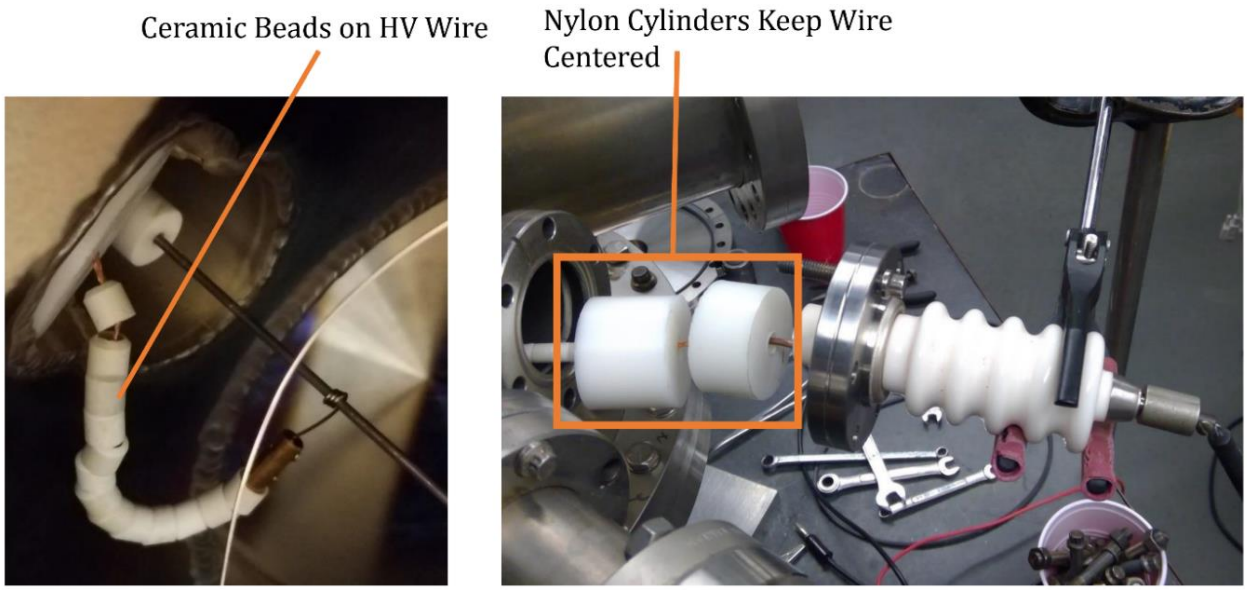

Figure 7. Insulation attempts for HV feedthrough. Ceramic beads were added to the HV wire as shown on the left. Since there were still issues with sparking, nylon cylinders were created to keep the wire entering the chamber as far as possible from the chamber walls as shown on the right.

1.3.3. Recent Progress

Since the power supply could no longer measure current, a device was created to measure both the current and the voltage. Furthermore, the entire remote operating system has been rewritten in python. The communication system no longer uses the ethernet framework but relies on USB to RS-232/RS-234 communication. Finally, first steps toward an automated control system for the pressure and HV have been implemented.

Chapter 2

PLASMA THEORY

Since the fusor works by confining a plasma, it is useful to examine the differential equations that govern the evolution of the charge and current density within the plasma as well as the resulting electric and magnetic fields generated by the plasma for a particular configuration of external electric and magnetic fields. The following description begins by considering the equations for individual particles, then employs averaging techniques to derive a second order differential equation that, when coupled with Maxwell's equations, completely describes the average properties of a plasma. The equations can then be solved for the charge and current density and the electric and magnetic fields by making some simplifying assumptions about the fusor configuration.

2.1. Description of a Plasma

2.1.1. Microscopic Description

Following the derivation by Callen [19], consider an individual particle, either an electron or an ion, at position in three-dimensional space $\mathbf{x}(t)$ at time t. Furthermore, using cartesian coordinates, it is clear $\mathbf{x}(\mathrm{t}) = [x(t), y(t), z(t)]$. Classically, the particle will be found at a single point in space. It follows then, that the spatial number distribution integrated over all of space is exactly one. Since the spatial distribution everywhere except at the point where the particle exists is zero, it follows that the spatial distribution is described by a 3-dimensional Dirac delta,

$$\delta[\mathbf{x} - \mathbf{x}(t)] = \delta[x - x(t)]\,\delta[y - y(t)]\,\delta[z - z(t)]. \tag{6}$$

Notice that evaluating the distribution function at location $\mathbf{x}$ for a particle with trajectory $\mathbf{x}(t)$ would result in zero everywhere except where the particle is at time t, for which at this location it is infinite. Since the Dirac delta distribution is only used within an integral, the distribution function should be integrated over three-dimensional space to have any meaning.

The velocity distribution is defined similarly. For a single particle with velocity $\mathbf{v}(t)$ the velocity distribution function is

$$\delta[\mathbf{v} - \mathbf{v}(t)] = \delta[v_x - v_x(t)]\,\delta\big[v_y - v_y(t)\big]\,\delta[v_z - v_z(t)], \tag{7}$$

where $\mathbf{v} = [\,v_x,\ v_y, v_z]$ is the location at which the velocity distribution function is being evaluated in velocity space. From these two distribution functions, a distribution function across all of phase space can be obtained. Summing over all particles, the microscopic distribution function, $f^m(\mathbf{x}, \mathbf{v}, t)$ is

$$f^m(\mathbf{x}, \mathbf{v}, t) = \sum_{i=1}^{N} \delta[\mathbf{x} - \mathbf{x}_i(t)]\,\delta[\mathbf{v} - \mathbf{v}_i(t)] \tag{8}$$

where N is the total number of particles and each particle is indexed by i. This describes the distribution of particles in six-dimensional phase space. The spatial particle density function, $n^m(\mathbf{x}, t)$, will simply be the spatial part of this, integrated over all velocities, v. That is

$$n^m(\mathbf{x}, t) = \int d^3v f^m(\mathbf{x}, \mathbf{v}, t) = \sum_{i=1}^{N} \delta[\mathbf{x} - \mathbf{x}_i(t)]. \tag{9}$$

Integrating the particle density function, $n^m(\mathbf{x}, t)$, over a volume yields the number of particles in the volume.

The microscopic trajectory of each particle is determined using Newton's second law. The force on each charged particle comes from the electric field $\mathbf{E}^m(\mathbf{x}_i, t)$ and magnetic field $\mathbf{B}^m(\mathbf{x}_i, t)$ created by the combination of other charged particles and any external fields present. The equation of motion for each particle is then given by the Lorentz force

$$m\frac{d\mathbf{v}_i}{dx} = q[\mathbf{E}^m(\mathbf{x}_i, t) + \mathbf{v}_i \times \mathbf{B}^m(\mathbf{x}_i, t)], i = 1,2, \dots, N \tag{10}$$

where m is the mass of a single particle. Maxwell's equations govern the electric and magnetic fields, so it will be useful to find the charge density and current density for the microscopic description of the plasma. Since ions and electrons have different charges, it is necessary to introduce an index for the species of the particle, s. The equation for charge density for a particular species will simply be the particle density multiplied by the charge for that species. It follows,

$$\rho_q^m(\mathbf{x},t) = \sum_s q_s \int d^3v f_s^m(\mathbf{x},\mathbf{v},t) = \sum_s q_s \sum_{i=1}^{N} \delta[\mathbf{x}-\mathbf{x}(t)] \tag{11}$$

where $\rho_q^m(\mathbf{x},t)$ is the microscopic charge density. The microscopic current density, $\mathbf{J}^m(\mathbf{x},t)$, will simply be the microscopic charge density multiplied by the velocity

$$\mathbf{J}^m(\mathbf{x},t) = \sum_s q_s \int d^3v \mathbf{v} f_s^m(\mathbf{x},\mathbf{v},t) = \sum_s q_s \sum_{i=1}^{N} \mathbf{v}_i \delta[\mathbf{x}-\mathbf{x}(t)]. \tag{12}$$

These equations, when combined with Maxwell's equations, completely describe a plasma as it evolves over time for an initial set of conditions. To obtain any useful information about the plasma though, a system of N differential equations would have to be solved. It is convenient then, to find some way to find the average properties of the ensemble.

2.1.2. Plasma Kinetic Equation

Before averaging the microscopic distribution function, it will be useful to find the derivative of the microscopic distribution function with respect to time. Using the multivariate chain rule, it can be shown that

$$\begin{aligned} \frac{df^m}{dt} &= \frac{d}{dt}\left(\sum_{i=1}^{N} \delta[\mathbf{x}-\mathbf{x}_i(t)]\,\delta[\mathbf{v}-\mathbf{v}_i(t)]\right) \\ &= \left(\frac{\partial}{\partial t} + \frac{d\mathbf{x}}{dt}\cdot\boldsymbol{\nabla}_{\mathbf{x}} + \frac{d\mathbf{v}}{dt}\cdot\boldsymbol{\nabla}_{\mathbf{v}}\right)\left(\sum_{i=1}^{N} \delta[\mathbf{x}-\mathbf{x}_i(t)]\,\delta[\mathbf{v}-\mathbf{v}_i(t)]\right). \end{aligned} \tag{13}$$

Because it is a property of the delta function when integrated over a volume that includes $\mathbf{x}_i$ that $\mathbf{x}\delta[\mathbf{x}-\mathbf{x}_i] = \mathbf{x}_i\delta[\mathbf{x}-\mathbf{x}_i]$, it follows that

$$\frac{df^m}{dt} = \left(\sum_{i=1}^{N}\left(\frac{\partial}{\partial t} + \frac{d\mathbf{x_i}}{dt}\cdot\boldsymbol{\nabla}_{\mathbf{x}} + \frac{d\mathbf{v_i}}{dt}\cdot\boldsymbol{\nabla}_{\mathbf{v}}\right)\delta[\mathbf{x}-\mathbf{x}_i(t)]\,\delta[\mathbf{v}-\mathbf{v}_i(t)]\right). \tag{14}$$

Taking just the partial derivative with respect to t, it becomes clear that,

$$\frac{df^m}{dt} = \left(\sum_{i=1}^{N}\left(-\frac{d\mathbf{x_i}}{dt}\cdot\boldsymbol{\nabla}_{\mathbf{x}} - \frac{d\mathbf{v_i}}{dt}\cdot\boldsymbol{\nabla}_{\mathbf{v}} + \frac{d\mathbf{x_i}}{dt}\cdot\boldsymbol{\nabla}_{\mathbf{x}} + \frac{d\mathbf{v_i}}{dt}\cdot\boldsymbol{\nabla}_{\mathbf{v}}\right)\delta[\mathbf{x}-\mathbf{x}_i(t)]\,\delta[\mathbf{v}-\mathbf{v}_i(t)]\right) = 0. \tag{15}$$

Equation (15) can be combined with Equation (10) to obtain a system of N equations, the total of which is

$$\frac{\partial f^m}{\partial t} + \boldsymbol{\nabla}_{\mathbf{x}} f^m \cdot \frac{d\mathbf{x}}{dt} + \boldsymbol{\nabla}_{\mathbf{v}} f^m \cdot \left[\frac{q}{m}[\mathbf{E}^m(\mathbf{x},t) + \mathbf{v}_i \times \mathbf{B}^m(\mathbf{x},t)]\right] = 0 \tag{16}$$

for a single species and charge state. This equation can now be averaged. Consider the particles inside a small, three-dimensional space box of volume ΔV and the small velocity-space volume ΔV_v. The number of particles $N_{6D} = \int_{\Delta V} d^3x \int_{\Delta V_v} d^3v f^m$ in this box should be large enough that the statistical fluctuations of particles within the box is small, but the box should also not be so large that the average properties of the plasma vary within it. To meet the first requirement, the box needs to be large compared to the average spacing of particles within the plasma, which is given by the inverse of the density function. That is, $\Delta V > 1/n$, where n is given in Equation (9). To meet the second requirement, each side of the box should be small compared to the Debye shielding length, λ_D, which is the length for which the electric field due to a charged particle is collectively shielded out due to the arrangement of surrounding charged particles. The Debye length is given by

$$\lambda_D = \left(\frac{4\pi n q^2}{k_B T}\right)^{-1/2} \tag{17}$$

where q is the charge of the species, T is the "temperature" of the system, and k_B, is the Boltzmann constant. The requirement for box size is then $n^{-1/3} < \Delta x < \lambda_D$. The average distribution function is then approximately,

$$\langle f^m \rangle = \lim_{n^{-1/3} < \Delta x < \lambda_D} \frac{N_{6D}}{\Delta V \Delta V_v} = \lim_{n^{-1/3} < \Delta x < \lambda_D} \frac{\int_{\Delta V} d^3x \int_{\Delta V_v} d^3v f^m}{\int_{\Delta V} d^3x \int_{\Delta V_v} d^3v}. \tag{18}$$

The difference between the distribution function and the average value of the distribution function will be written as δf^m where,

$$\delta f^m = f^m - \langle f^m \rangle. \tag{19}$$

To understand the difference between the microscopic distribution function and the average distribution function examine Figure 8 where two example distribution functions are plotted for position in one dimension.

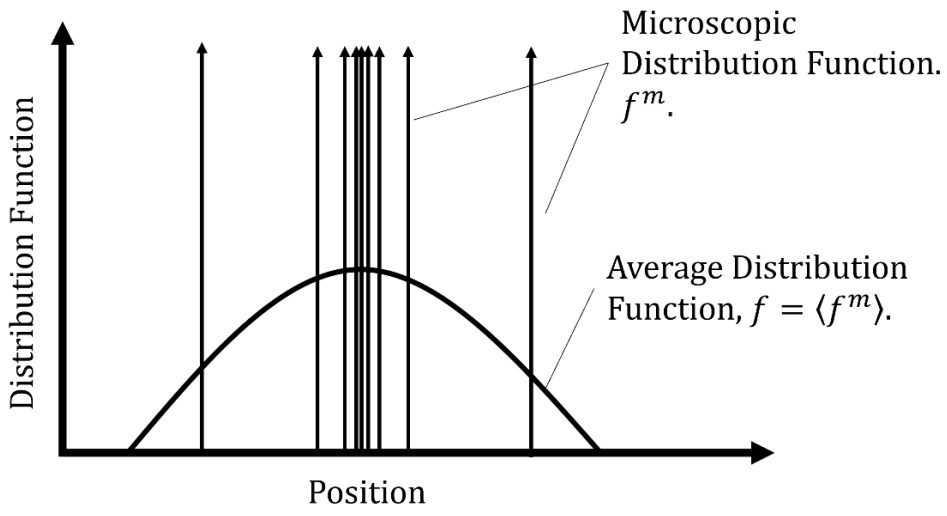

Figure 8. Microscopic and average distribution function in one dimension. The spikes in the microscopic distribution correspond to each particle and the integral of the function across all of position space will be the total number of particles, *N*. While the average distribution function is smoothed, the integral of it across position space, corresponding to the area under the curve, will also be *N*.

The microscopic distribution is spikey, corresponding to the Dirac delta for each particle, while the average distribution function is smooth. Recall though that since the Dirac delta only makes sense in the context of integrating over a volume, when integrating both distribution functions over position, the result will be the number of particles, *N*, in the volume.

The smoothed average of the electric and magnetic fields as well as the charge density and current density can be defined the same way as the smoothed average of the distribution function. That is,

$$\mathbf{E}^m = \langle \mathbf{E}^m \rangle + \delta \mathbf{E}^m, \qquad \mathbf{B}^m = \langle \mathbf{B}^m \rangle + \delta \mathbf{B}^m, \tag{20}$$
$$\rho_q^m = \langle \rho_q^m \rangle + \delta \rho_q^m, \qquad \text{and} \quad \mathbf{J}^m = \langle \mathbf{J}^m \rangle + \delta \mathbf{J}^m .$$

Notice, that by definition, $\langle \delta f^m \rangle = 0$ since this is the average of the differences between the true value and the average value. The same is true for the other functions. Inserting these definitions into Equation (16),

$$\frac{\partial \langle f^m \rangle}{\partial t} + \boldsymbol{\nabla}_{\mathbf{x}} \langle f^m \rangle \cdot \mathbf{v} + \boldsymbol{\nabla}_{\mathbf{v}} \langle f^m \rangle \cdot \left[\frac{q}{m} [\langle \mathbf{E}^m \rangle + \mathbf{v} \times \langle \mathbf{B}^m \rangle] \right] = -\frac{q}{m} \langle [\delta \mathbf{E}^m + \mathbf{v} \times \delta \mathbf{B}^m] \cdot \boldsymbol{\nabla}_{\mathbf{v}} \langle f^m \rangle \rangle. \tag{21}$$

This is the fundamental plasma kinetic equation, and is usually written,

$$\frac{\partial f}{\partial t} + \mathbf{v} \cdot \boldsymbol{\nabla}_{\mathbf{x}} f + \boldsymbol{\nabla}_{\mathbf{v}} f \cdot \left[\frac{q}{m} [\mathbf{E} + \mathbf{v} \times \mathbf{B}] \right] = C(f) \tag{22}$$

where $\langle f^m \rangle$ is defined as the smoothed average distribution function f. Similarly, **E** and **B** are the smoothed average $\langle \mathbf{E}^m \rangle$ and $\langle \mathbf{B}^m \rangle$ respectively. The term on the right, $C(f)$, represents the coulomb collision effects on the average distribution function.

The four Maxwell equations in gaussian units, where *c* is the speed of light in a vacuum,

$$\boldsymbol{\nabla} \cdot \mathbf{E} = 4\pi \rho_q, \tag{23}$$

$$\boldsymbol{\nabla} \times \mathbf{E} = -\frac{1}{c} \frac{\partial \mathbf{B}}{\partial t}, \tag{24}$$

$$\nabla \cdot \mathbf{B} = 0, \tag{25}$$

$$\text{and} \quad \nabla \times \mathbf{B} = \frac{1}{c}\left(4\pi\mathbf{J} + \frac{\partial \mathbf{E}}{\partial t}\right) \tag{26}$$

along with the charge density and current density functions,

$$\rho_q(\mathbf{x}, t) = \sum_s q_s \int d^3v f_s(\mathbf{x}, \mathbf{v}, t), \tag{27}$$

and

$$\mathbf{J}(\mathbf{x}, t) = \sum_s q_s \int d^3v \mathbf{v} f_s(\mathbf{x}, \mathbf{v}, t), \tag{28}$$

coupled with Equation (22) provide a complete, albeit difficult to solve, description of a plasma. Some simplifying assumptions can be made to solve for the various properties of a plasma.

2.2. Plasma Description in an IEC Device

For a basic description of a fusor such as the one at Houghton, consider the plasma to be in a stable equilibrium and possess an electrode configuration with spherical symmetry. From symmetry arguments, **v** only depends on *r* and only has a radial component. That is, the velocity is given as $\mathbf{v} = v(r)$, and it follows that the fundamental distribution function *f* is a function of $v(r)$ and r only. Furthermore, since the system is in equilibrium, it has no explicit time dependence. Finally, the collisional effects, $C(f)$, are assumed to be negligible, so $C(f) = 0$. When this last assumption is made, the fundamental plasma kinetic equation becomes

$$\frac{\partial f}{\partial t} + \mathbf{v} \cdot \nabla_{\mathbf{x}} f + \nabla_{\mathbf{v}} \cdot f\left[\frac{q}{m}[\mathbf{E} + \mathbf{v} \times \mathbf{B}]\right] = 0. \tag{29}$$

Equation (29) is known as the Vlasov equation. Because of the spherical symmetry, it is clear $\mathbf{B} = 0$ and $\mathbf{E} = E(r)\hat{\mathbf{r}}$. It is simple to see why this is the case, because **B** does not have any component in the radial direction, and if **B** had a component in any other direction, simply rotating the system about an axis would immediately change **B,** meaning the system

would not have spherical symmetry. Using this, as well as the fact $f = f(r, v(r))$, the Vlasov equation further reduces to

$$\frac{\partial f}{\partial r} v + \frac{\partial f}{\partial v}\left(\frac{qE}{m}\right) = 0. \tag{30}$$

Rearranging, Equation (30) gives

$$\frac{\partial f}{\partial r} m v_r = -\frac{\partial f}{\partial v_r}(qE_r). \tag{31}$$

Integrating with respect to v and r, it is found,

$$\frac{1}{2} m v^2 = -qV + \varepsilon, \tag{32}$$

where qV is potential energy and ε is an integrating constant. Notice the left side of this equation describes the kinetic energy of the particles and the right side describes the potential energy. It follows that ε is the total energy of the particles.

Equation (32) allows for the relationship used by Elmore et. al. [12] to be easily obtained. This follows because Equation (32) becomes two different equations when the charge of the particle is put in for q. The equation for the electrons is

$$\frac{1}{2} m_e {v_e}^2 - eV = \varepsilon_{0e} \tag{33}$$

where m_e is the mass of the electrons and v_e is the velocity of the electrons. Similarly, the equation for the positively charged ions is

$$\frac{1}{2} m_i {v_i}^2 + eV = \varepsilon_{0i} \tag{34}$$

where m_i is the mass of the ions and v_i is the velocity of the ions.

Recall Poisson's equation when using Gaussian units,

$$\boldsymbol{\nabla}^2 V = -4\pi\rho. \tag{35}$$

Because of spherical symmetry, the potential only depends on the distance from the cathode, *r*, and the total charge density will be the ion density minus the electron density, Equation (35) becomes

$$\frac{1}{r^2}\frac{\partial}{\partial r}\left(r^2\frac{\partial V}{\partial r}\right) = -4\pi[\rho_i - \rho_e]\,. \tag{36}$$

Since the current, *I,* is

$$I = \int \mathbf{J}\cdot d\mathbf{A} = \int \rho\mathbf{v}\cdot d\mathbf{A} \tag{37}$$

where **A** is the area vector normal to the enclosed surface, it follows, since the electron current will be going both inward and outward equally, the electron current directed either inward or outward is one half the total current. It is convenient to integrate over a sphere since the particles are all directed radially. It follows

$$I_e = \frac{1}{2}\int_0^{2\pi}\int_0^{\pi}\rho_e v_e\, r^2 \sin\theta\, d\theta d\phi = 2\pi\rho_e v_e r^2 \tag{38}$$

since **v** and ρ are a function of *r* only. Similarly, the ion current is

$$I_i = \frac{1}{2}\int_0^{2\pi}\int_0^{\pi}\rho_i v_i\, r^2 \sin\theta\, d\theta d\phi = 2\pi\rho_i v_i r^2. \tag{39}$$

Following the derivation done by Elmore et. al. [12] it is useful to introduce the dimensionless variable *W*, where

$$W = \frac{\frac{1}{2} m_e {v_e}^2}{\Lambda} \tag{40}$$

and Λ is a constant determined later. By solving Equation (40) for v_e, It follows immediately

$$v_e = \left(\frac{2\Lambda W}{m_e}\right)^{\frac{1}{2}}. \tag{41}$$

Solving Equation (34) for v_i yields

$$v_i = \left(\frac{2(\varepsilon_{0i} - eV)}{m_i}\right)^{\frac{1}{2}}. \tag{42}$$

Notice Equation (33) can be written as

$$-eV = \varepsilon_{0e} - \frac{1}{2} m_e {v_e}^2 . \tag{43}$$

Combining Equations (42) and (43), it is found that

$$v_i = \left(\frac{2[\varepsilon_{0e} + \varepsilon_{0i} - \frac{1}{2} m_e {v_e}^2]}{m_i}\right)^{\frac{1}{2}}. \tag{44}$$

Equation (44) can be written as

$$v_i = \left(\frac{2\Lambda[W_o - W]}{m_i}\right)^{\frac{1}{2}} \tag{45}$$

where

$$W_o = \frac{1}{\Lambda}[\varepsilon_{0e} + \varepsilon_{0i}]. \tag{46}$$

Notice Equations (38) and (39) can be solved for ρ_e and ρ_i respectively. It follows

$$\rho_i - \rho_e = \frac{I_i}{2\pi v_i r^2} - \frac{I_e}{2\pi v_e r^2}. \tag{47}$$

Inserting Equations (41) and (45) into (46) it is found

$$4\pi[\rho_i - \rho_e] = \frac{2I_i}{\left(\frac{2\Lambda[W_o - W]}{m_i}\right)^{\frac{1}{2}} r^2} - \frac{2I_e}{\left(\frac{2\Lambda W}{m_e}\right)^{\frac{1}{2}} r^2}. \tag{48}$$

This can be rewritten as

$$4\pi[\rho_i - \rho_e] = \frac{2}{r^2}\left[\frac{I_i m_i^{\frac{1}{2}}}{(2\Lambda[W_o - W])^{\frac{1}{2}}} - \frac{I_e m_e^{\frac{1}{2}}}{(2\Lambda W)^{\frac{1}{2}}}\right]. \tag{49}$$

Finally, it is seen that

$$4\pi e[\rho_i - \rho_e] = -\frac{2eI_e}{\left(\frac{2\Lambda}{m_e}\right)^{\frac{1}{2}} r^2}\left[\frac{1}{W^{\frac{1}{2}}} - \frac{G_0}{[W_0 - W]^{\frac{1}{2}}}\right] \tag{50}$$

where

$$G_0 = \frac{I_i}{I_e}\left(\frac{m_i}{m_e}\right)^{\frac{1}{2}}. \tag{51}$$

Combining Equations (44) and (36), it is found

$$\frac{\partial}{\partial r}\left(r^2 \frac{\partial W}{\partial r}\right) = \frac{1}{W^{\frac{1}{2}}} - \frac{G_0}{[W_0 - W]^{\frac{1}{2}}}. \tag{52}$$

It is convenient to define Λ as

$$\Lambda^{\frac{1}{2}} = \sqrt{2} e I_e (m_e)^{\frac{1}{2}} \tag{53}$$

so that a new variable, z, can be introduced to simply the equation. This variable is set to be

$$\mathrm{z} = \ln \frac{r}{r_0}. \tag{54}$$

where r_0 is considered to be the characteristic "width" of the central region which comes from setting the boundary conditions

$$\frac{\partial W}{\partial z} = 0 \text{ for } \mathrm{z} = 0. \tag{55}$$

Introducing these variables allows Equation (46) to be written as

$$\frac{d^2 W}{dz^2} + \frac{dW}{dz} = \frac{1}{W^{\frac{1}{2}}} - \frac{G_0}{[W_0 - W]^{\frac{1}{2}}}. \tag{56}$$

Elmore et. al. found that when G_0 was zero, solutions to this equation indicate a practical system for creating a potential well is feasible. When G_0 is not zero though, it is clear integrating from $z = 0$ on the right, which corresponds to $r = r_0$, will result in W getting larger, but never reaching W. This means the second term in equation (5) will dominate, meaning the potential never becomes large enough to confine the ions. According to Elmore et. al. this difficulty arises from the faulty assumption that all ions are injected with a single energy ε_o. If instead the ions are injected with a radial Maxwell distribution, which is optimistic for the successful confinement of the device, the density becomes

$$n(r) = n_0 r_0^2 \frac{\exp\left(-\frac{W_e}{\rho}\right)}{r^2} \tag{57}$$

This will replace Equation (53) with

$$\frac{d^2 W_e}{dz^2} + \frac{dW_e}{dz} = \frac{1}{W_e^{\frac{1}{2}}} - G \exp\left(-\frac{W_e}{\rho}\right) \tag{58}$$

where

$$G = \frac{2\pi n_0 e r_0^2}{I_e}\left(\frac{2\Lambda}{m_e}\right)^{\frac{1}{2}}. \tag{59}$$

Equation (59) is useful in calculating the maximum thermonuclear power of an IEC device. For more discussion, see the derivation done by Miley et. al. [3].

Chapter 3

EXPERIMENT AND DEVICE DESCRIPTION

The IEC experiments conducted at Houghton University used an ion injected Farnsworth-Hirsch fusor, which is shown in Figure 9. A detailed description of the vacuum system, the gas handling system, the high voltage system, and the control system are described in this chapter. Basic experiments to determine calibration data for the mass flow controller as well as the current measurement device are also described.

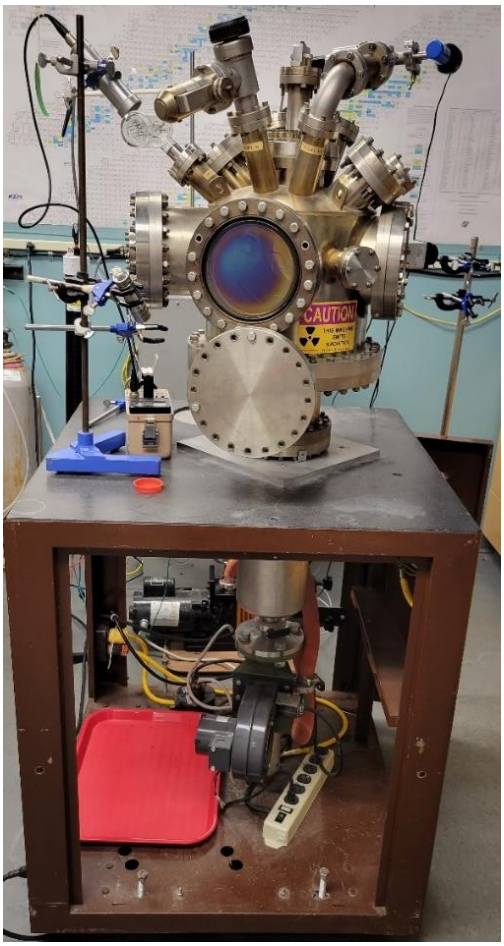

Figure 9. Photograph of the Houghton Fusor. The large stainless-steel vacuum chamber sits atop a metal cart containing the vacuum pumps used to evacuate the chamber. Many ports allow pressure gauges, a mass flow controller, electrical feedthroughs, and viewports to be attached to the chamber.

3.1. Vacuum System Overview

The frame of the Houghton fusor consists of a large, stainless-steel chamber atop a cart. The chamber is a 0.35 meter diameter roughly cylindrical steel chamber that has 18 ports. These ports have conflat flanges (CF). Some of these ports are used for attaching instruments to the chamber or as a viewport, while many not needed ports are closed off with steel conflat flange blanks using rubber CF O-rings to seal the ports. Table 1 provides a description of each port, numbered according to the diagrams shown in Figure 10.

Table 1. Description of fusor ports. The ports are numbered according to the labeling in Figure 10.

Port Number	Description
1	2.75" CF adapted to 1.33" CF for HV feedthrough for interior HV electrode grid
2	Linear motion feedthrough 2.75 CF for interior HV electrode grid
3	8" CF blank
4	2.75" CF with Varian Model L6280-301 angle valve to Apex AX-MC-50SCCM-D Flow Controller
5	8" CF viewport
6	2.75" CF blank
7	8" CF viewport with 8" CF blank steel shield covering the glass aperture
8	8" CF port adapted to 2.75" CF blank
9	2.75" CF to Kurt. J. Lesker G100F hot cathode ion gauge tube
10	4" CF blank
11	2.75" CF blank
12	2.75" CF blank
13	2.75" CF blank
14	4" CF blank
15	2.75" CF with 90° elbow to quick flange tee attached to Kurt J. Lesker 275806 pirani gauge and 925 MicroPirani vacuum pressure transducer.
16	2.75" CF with Varian Model 951-5013 angle valve to Varian variable leak valve model 951-5100
17	6" CF port adapted to 2.75" CF with linear motion feedthrough for the grounded electrode and the ground electrode output
18	14" CF connected to vacuum pumps through cold trap

Within the chamber, the cathode for the IEC is a 7-cm-diameter sphere consisting of three wire rings made of 0.63-mm-diameter 304 stainless steel wire spot welded together such that each ring is oriented orthogonally to the others. This is shown at A in Figure 11. The

spherical grid is spot welded to a Du-Bro 173 2-56 steel threaded rod, C, that is attached to a linear motion feedthrough connected to port 2, allowing the position of the spherical cathode grid to be adjusted within the vacuum chamber. A spherical electrode is similarly constructed from two 20-cm-diameter rings and two 15-cm-diameter rings as shown at B in Figure 11. This hangs from a linear motion feedthrough at the top of the vacuum chamber through port 17.

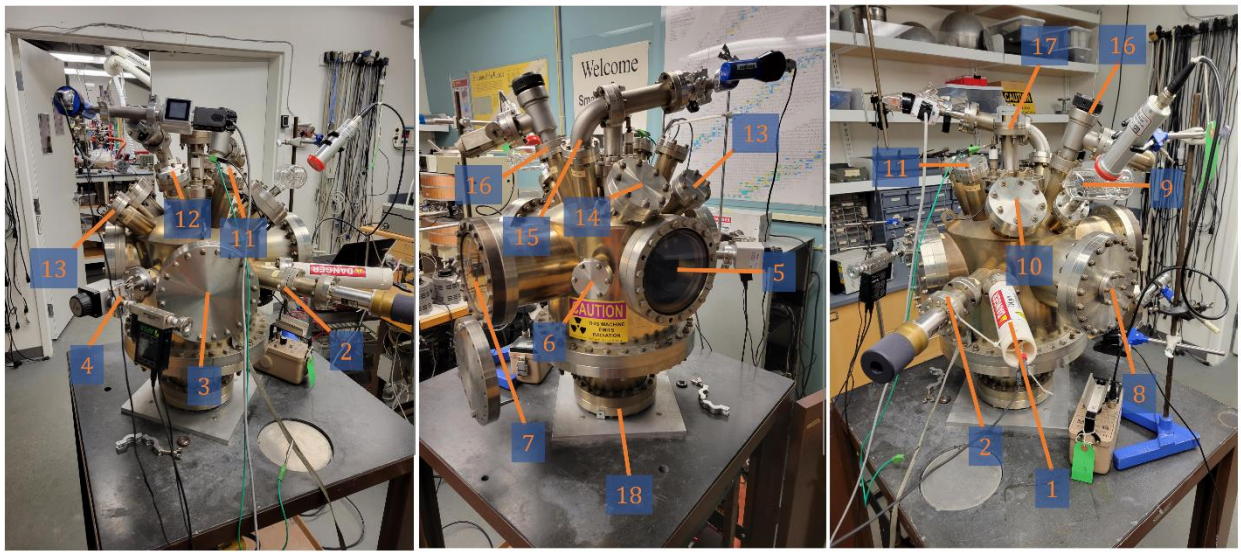

Figure 10. Fusor from three angles with numbered ports. There are 18 conflat flange style ports to the vacuum chamber in total. These are used as viewports and electrical feedthroughs as well as gas, vacuum, and gauge connections, or they are closed off.

The chamber is mounted on top of the cart such that a hole in the top of the cart aligns with a 0.35-m-diameter CF opening at the bottom of the vacuum chamber. This opening connects to a reducer which connects to an 8" CF port, to which the pump system is attached. The air within the vacuum chamber is rough pumped with an Altec 2008A rotary fore pump which brings the pressure in the chamber down to the low 10^{-3} Torr range. An air-cooled Varian model 1059 diffusion pump connected in series with the fore pump as shown in Figure 12 is then turned on which further evacuates the chamber to the low 10^{-6} Torr range. A Kurt J. Lesker model #TLR6XS150QF liquid nitrogen cold trap is placed between the diffusion pump and the chamber. This allows the chamber to get to as low as 10^{-7} Torr [17], but since these

pressures were not required, the trap was not used for the experiments described in this thesis.

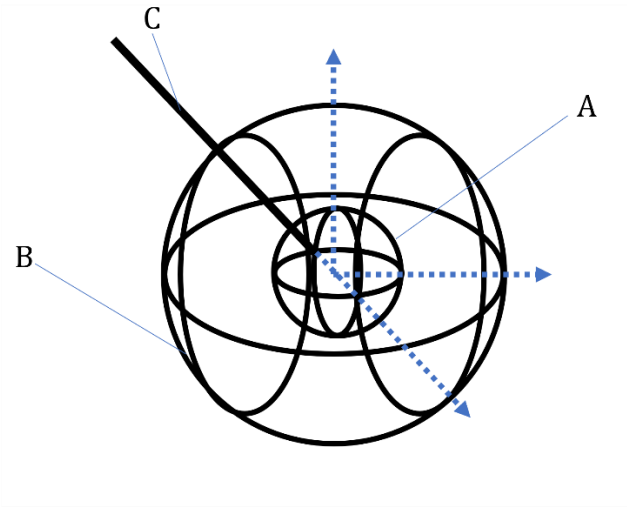

Figure 11. Diagram of spherical wire grids. A small inner sphere A made up of three equally sized rings is attached to a rod C and acts as the physical cathode for the IEC device. A larger wire grid B consists of four rings of two different sizes and acts as the grounded electrode for the IEC device. A cartesian coordinate system was superimposed on this graphic to help visualize the configuration in 3D space.

3.2. Gas Handling System

A Varian Model L6280-301 angle valve between an Apex AX-MC-50SCCM-D flow controller and the chamber allowed for a gas to be introduced to the chamber at varying rates if the manual valve was opened. Though any gas could be connected to the mass flow controller via a quick flange port, for all experiments described in this thesis, only air was introduced into the chamber. There are three pressure gauges attached to the chamber, each with a different range of operation. A Kurt. J. Lesker G100F hot cathode ion gauge measures pressures in the 10^{-5} to 10^{-6} Torr range using a Stanford Research Systems IGC100 controller. For most of the experiments, pressures are much higher than the allowed range of the hot cathode ion gauge, so a MKS Granville-Phillips 925 MicroPirani vacuum pressure transducer is used which measures pressures from 10^{-5} Torr to atmosphere. For comparison the purpose of comparison at higher pressures, a Kurt J. Lesker 275806 pirani gauge is attached to the chamber as well.

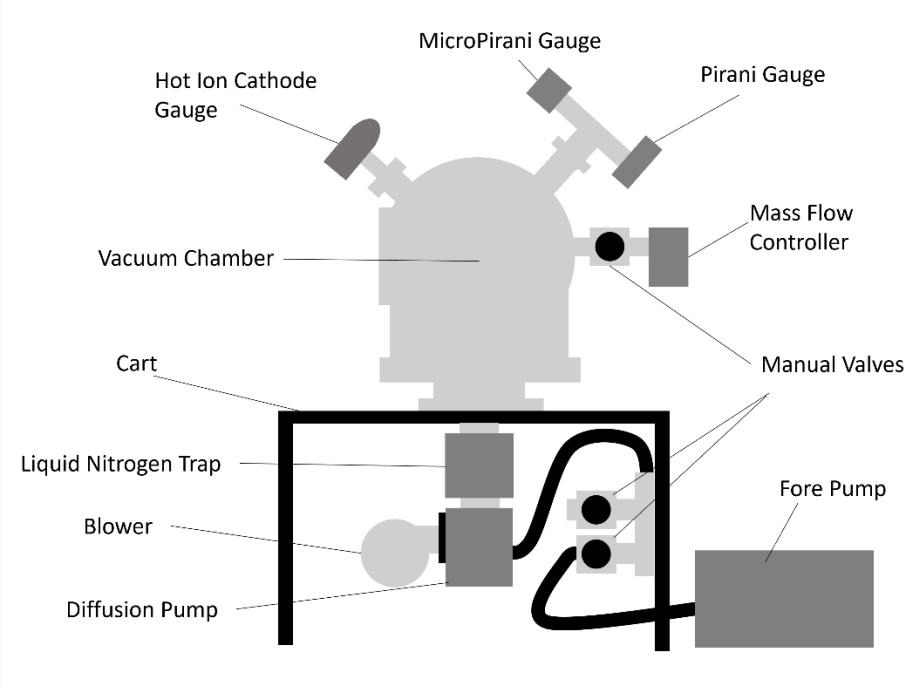

Figure 12. Gas system diagram for fusor. The vacuum chamber which is positioned on top of a cart is evacuated via a fore pump and an air-diffusion pump. The mass flow controller changes the pressure in the chamber by introducing a gas into the chamber at a specified rate if a manual valve opened. A hot ion cathode gauge, a microPirani gauge, and a Pirani gauge are used to measure the pressure for different ranges.

For confining a plasma, it is important to be able to accurately predict the chamber pressure for a particular set point of the mass flow controller. Pressures were measured using the microPirani gauge for various mass flow controller set points for air as shown in Figure 13. As can be seen, the correlation between the mass flow rate and the pressure within the chamber is nearly linear. Using a linear fit in Microsoft Excel, the equation

$$P = \text{Flow Rate} \times \left(0.0013 \frac{\text{Torr}}{\text{sccm}}\right) + 10^{-4}\ \text{Torr}$$

was obtained with an R^2 Value of 0.9933. Figure 14 shows the same linear fit using a log scale to demonstrate the linear fit is accurate for the lower pressure range.

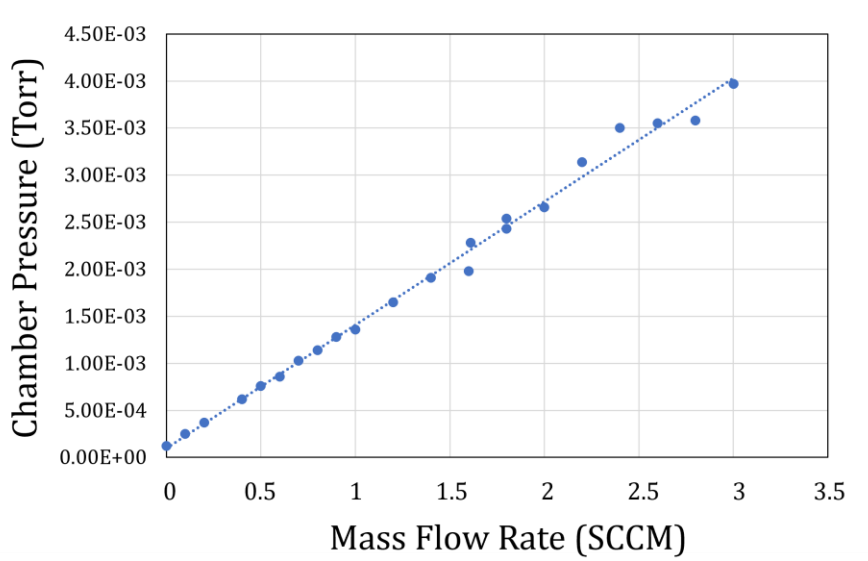

Figure 13. Plot of chamber pressure vs. mass flow rate of air. The pressure within the chamber increases nearly linearly with the mass flow rate.

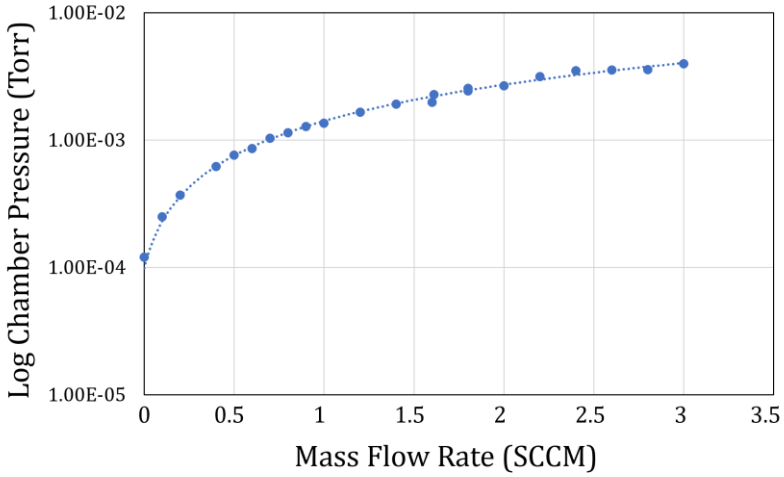

Figure 14. Log of chamber pressure vs. mass flow rate. Notice the linear fit is accurate for the lower pressure range.

When these calibration data were taken, to better understand the true pressure within the chamber, the hot cathode ion gauge was used when the chamber was at its lowest pressure, which corresponds to when the mass flow controller was set to zero. At this point, the hot cathode ion gauge pressure was measured to be 3.2×10^{-6} Torr, which was significantly

different than the MicroPirani gauge, which measured 1.1×10^{-4} Torr. The MicroPirani Gauge was also compared to the Pirani gauge at various pressures as shown in Figure 15. The measurements were similar for higher pressures, but less consistent for lower pressures. This aligns with the expectation that the MicroPirani would be more accurate at lower pressures. Since the microPirani gauge measurements were proportional to the Pirani gauge measurements, and the gauge continued to go down for lower pressures, the microPirani gauge was used for all experiments with the understanding that it may not be an accurate absolute measurement of pressure.

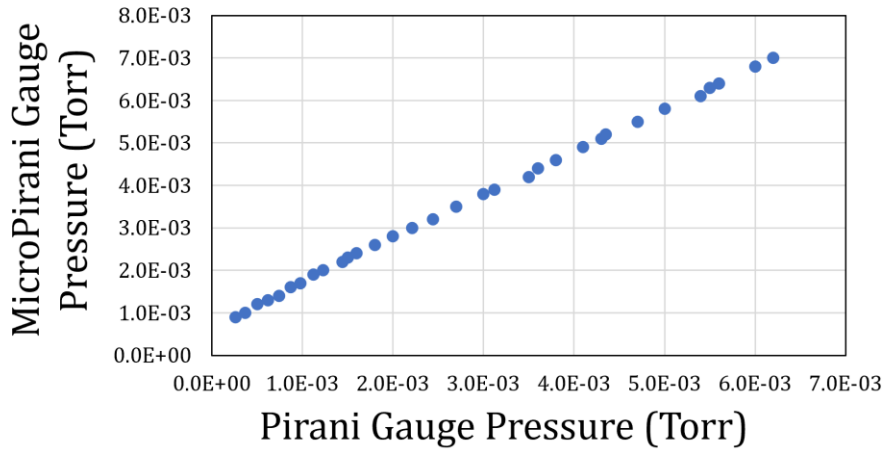

Figure 15. Pressure measured by Micro Pirani gauge vs. Pirani gauge. Notice the plot is nearly linear. The Micro Pirani gauge is expected to be more accurate at lower pressures than the Pirani gauge. Notice the measurements are similar for the higher pressures.

3.3. HV System

The negative high voltage applied to the inner electrode is supplied by a Bertan Series 815 - N high voltage power supply, as shown in Figure 16. The power supply is connected to a "homebuilt" device for measuring current flowing from the inner electrode to the HV power supply, and the voltage between the HV power supply output and ground. This device is connected to a 1.5 MΩ 7-watt ballast resistor, which is attached to the cathode. The ballast resistor is responsible for causing a drop in voltage when the current increases.

This serves to lower the current when the current becomes large, such as when sparking occurs.

3.3.1. Current and Voltage Measurement Device Circuitry

The current measurement aspect of the device is shown in the orange part of Figure 16. The conventional current flowing from the cathode into the -HV power supply passes through a WP710A10LGD LED. The LED light travels through a fiber-optic cable and is measured with a TEPT5700 NPN phototransistor. The phototransistor circuit acts as a voltage divider between +5V and ground, were the small voltage across a 100-kΩ resistor is amplified and measured, corresponding to different currents flowing through the phototransistor.

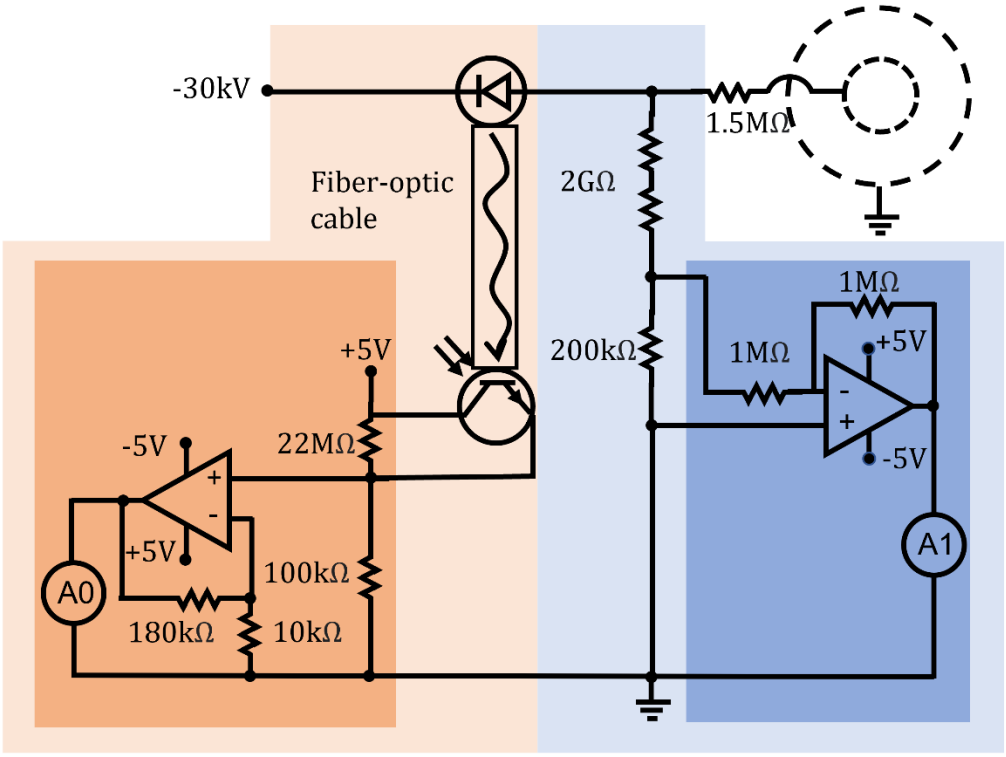

Figure 16. Schematic of the current (orange) and voltage (blue) measurement device. The current is measured using the light from an LED, which travels through a fiber-optic cable, is measured with a phototransistor, amplified 19 times (dark orange), and read with an Arduino. The voltage is measured using a voltage divider. The voltage across a small resistor is inverted with a voltage follower circuit (dark blue) and measured with an Arduino.

A 22-MΩ resistor connects the +5V to the 100-kΩ resistor preventing the current from flowing in the opposite direction of the amplification circuit when there is no light to the phototransistor. The amplification circuit consists of an LM741 op-amp connected to a 10-kΩ resistor and a 180-kΩ resistor as shown in Figure 16, resulting in x19 amplification. This amplified voltage output is measured using pin A0 on an Arduino Uno.

The voltage supplied by the HV power supply is measured using a voltage divider as shown in the blue region of Figure 16. The resistor chain consists of four 500-MΩ resistors in series with a 200-kΩ resistor. The voltage across the small resistor is inverted since the power supply produces a negative voltage. This is done using an LM741 inverting voltage follower op amp circuit which uses two 1-MΩ resistors and the same power supply used in the amplifier for the current measurement. The inverted voltage is then measured using pin A1 on the Arduino Uno.

3.3.2. Current and Voltage Measurement Device Construction

The core of the voltage and current measurement device is contained within a 3-inch diameter PVC pipe measuring 67 cm long. To keep the device light tight so as not to affect the phototransistor measurement, the pipe, shown in Figure 17, is wrapped in black electrical tape and has two PVC screw-on cleanout plugs on either end.

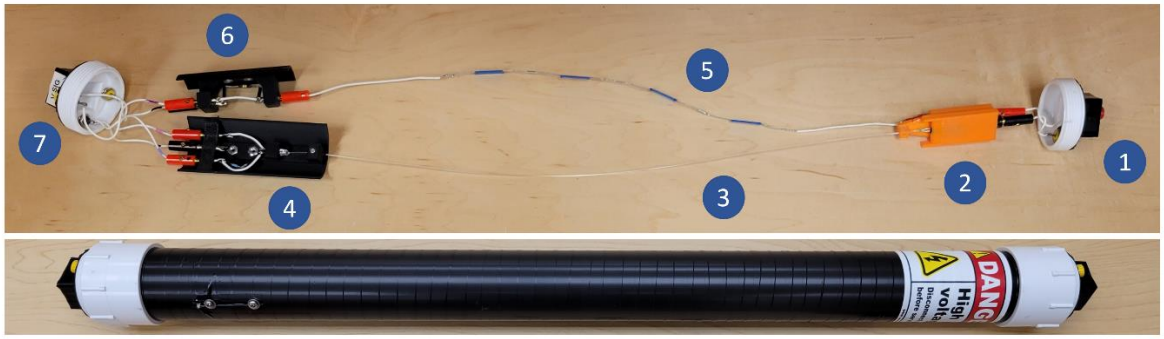

Figure 17. Voltage measurement device innerworkings. The voltage divider and phototransistor circuits are contained within a PVC pipe. The input terminals are attached to the PVC cap shown at 1 which connect to a 3D printed part, 2, that holds the LED light and fiber-optic cable, 3, as well as the resistor chain, 5. Both the phototransistor circuit holder, 4, and the voltage divider circuit holder, 6, can be adjusted within the PVC pipe to keep the fiber-optic cable and resistor chain extended within the pipe. The circuit is accessed through banana connectors attached to the PVC cap at 7.

Two holes are drilled into one of the caps and female banana connectors are screwed on as shown at 1 on Figure 17. When in operation, these sockets connect to the negative HV terminal of the power supply and the cathode of the fusor with banana plugs. A 3D printed part shown at 2 in Figure 17 as well as on the left side of Figure 18, houses the LED and connects to the terminals of the pipe as well as the resistor chain, shown at 5 in Figure 17. The LED is attached to a 0.75-mm-diameter fiber-optic cable, shown at 3 in Figure 17, using two-part epoxy. A small set screw on the 3D printed part helps hold the fiber-optic cable in place. The 3D printed part stays in place within the pipe with a 3D printed hook that is bolted onto the side of the pipe as shown on the right of Figure 18.

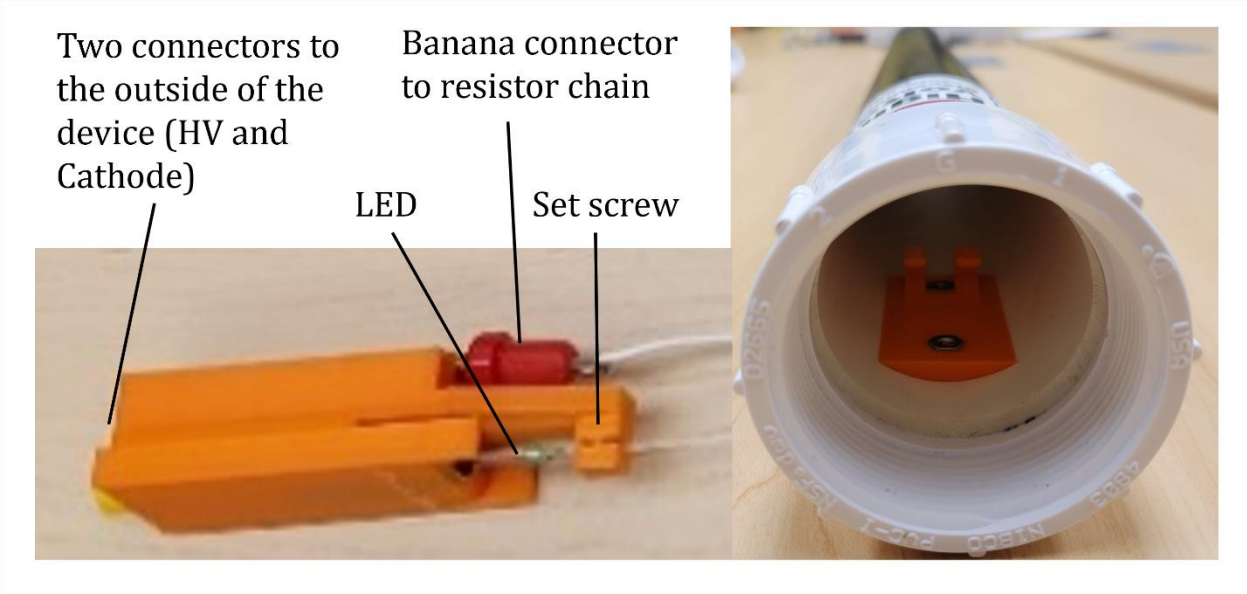

Figure 18. 3D printed LED holder and hook. The part on the left slides into the PVC pipe and catches on the hook attached to the PVC pipe on the right. The LED light is attached to the part on the left and a set screw holds a fiber-optic cable in place. A banana connector is used to attach the resistor chain as well as the negative HV and cathode connections.

At the other end of the fiber-optic cable, another 3D printed part, shown at 4 in Figure 17 as well as Figure 19, holds the components of the phototransistor circuit. A set screw is used to hold the fiber-optic in place. To keep the fiber-optic cable taught within the pipe, a slit was milled into the side of the PVC pipe. This slit allows the position of the phototransistor circuit holder to be adjusted along the length of the pipe by loosening small bolts.

Figure 19. 3D printed phototransistor circuit holder. The set screw, seen on the left, hold the fiber-optic cable in place. A phototransistor attaches to the resistor as well as the inputs for +5V and ground. The third input is the voltage to be measured across the resistor. The two nuts on the right side of the part allow bolts to screw into them so the part can be loosened and slid along a slit in the PVC pipe.

Similarly, a 3D printed part shown at 6 in Figure 17 as well as Figure 20, holds the components of the voltage divider circuit. A slit opposite the one used for the phototransistor circuit holder was milled into the side of the pipe to allow the position of the voltage divider circuit holder to be similarly adjusted. This keeps the resistor chain extended within the pipe, preventing it from touching the walls.

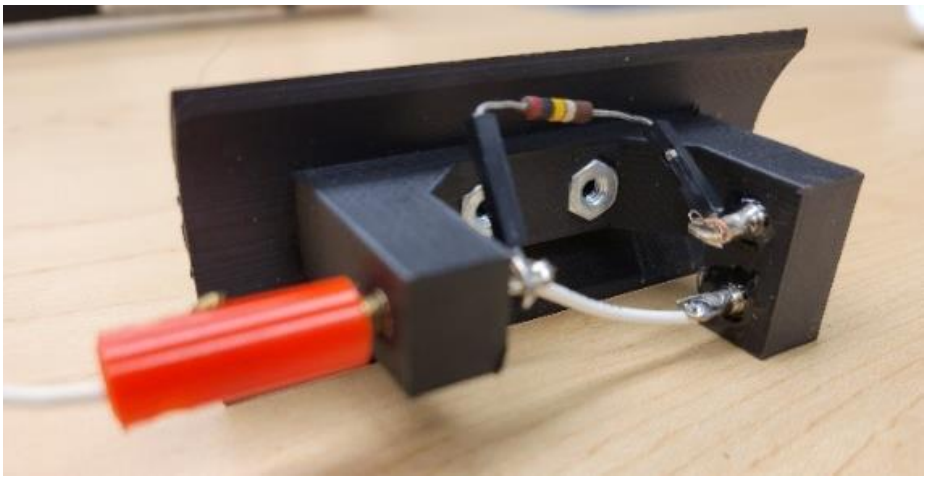

Figure 20. 3D printed voltage divider holder. The two nuts allow bolts to screw into them so the part can be loosened and slid along a slit in the PVC pipe. The red banana connector shown goes to the resistor chain. One of the other sockets connects to ground while the remaining one is the voltage to be measured.

The PVC plug at 7 in Figure 17 has four banana sockets screwed onto it. These are for a +5V input, ground, and the signal readout for both the phototransistor circuit and voltage divider. These sockets are connected to banana sockets on a 3D printed box, shown on the right of Figure 21, containing the two op-amp circuits described in the previous section. This box containing the op-amp circuits plugs directly into the Arduino UNO by simply placing it on top. A 3D printed part was created to connect the Arduino to the bottom of the PVC Pipe. The entire configuration can be observed on the left side of Figure 21. The op-amp circuit box is connected to ground, +5V, -5V, and the four outputs from the PVC tube. The Arduino can be queried by the computer for the voltage and current measurements.

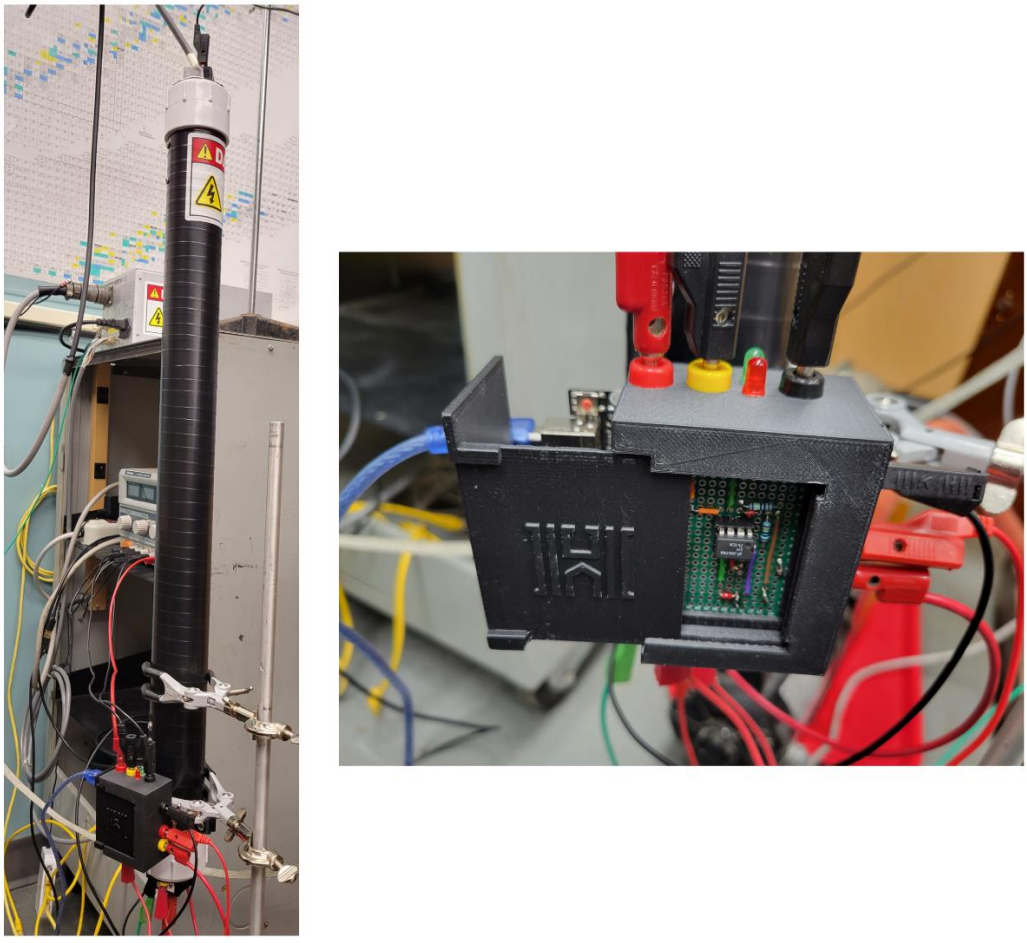

Figure 21. Voltage and current measurement device pictures. On the left is the device held with a ring stand. On the right is the op-amp circuit box plugged into the Arduino attached to the PVC pipe.

3.3.3. Calibration Data and Code

The voltage output by the HV power supply was determined by multiplying the voltage measured across the small resistor by the total resistance of the chain divided by the resistance of the smaller resistor. Though this was the method used in all experiments, an initial experiment comparing the set voltage of the HV power supply vs. the voltage measured by the device suggests this may not be accurate. Figure 22 shows the measured voltage of the device converted using the calculation from the resistors for various set points of the HV power supply with a linear fit.

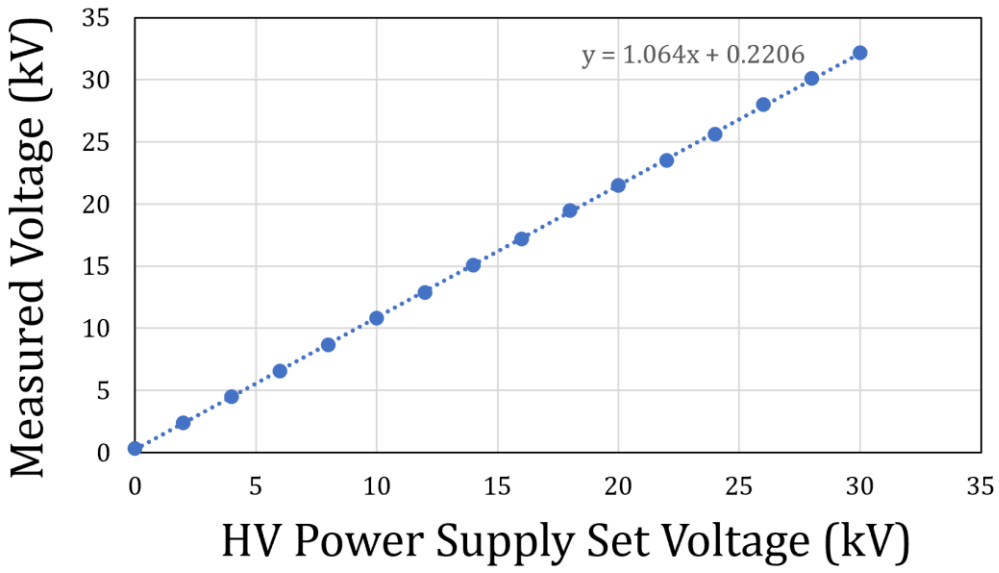

Figure 22. Set voltage of power supply vs. measured voltage from device.
Notice the set voltage is always slightly lower than the measured voltage.

To determine the current flowing out of the HV electrode based on the amount of light measured by the phototransistor and amplification circuit, a current was passed through the LED with an ammeter connected in series, and the raw analog input of the Arduino was measured as the current was raised. Plotting ammeter current against the Arduino input, a fourth-degree polynomial was fit for the purpose of interpolating the current based on the analog input. This fit is shown in Figure 23.

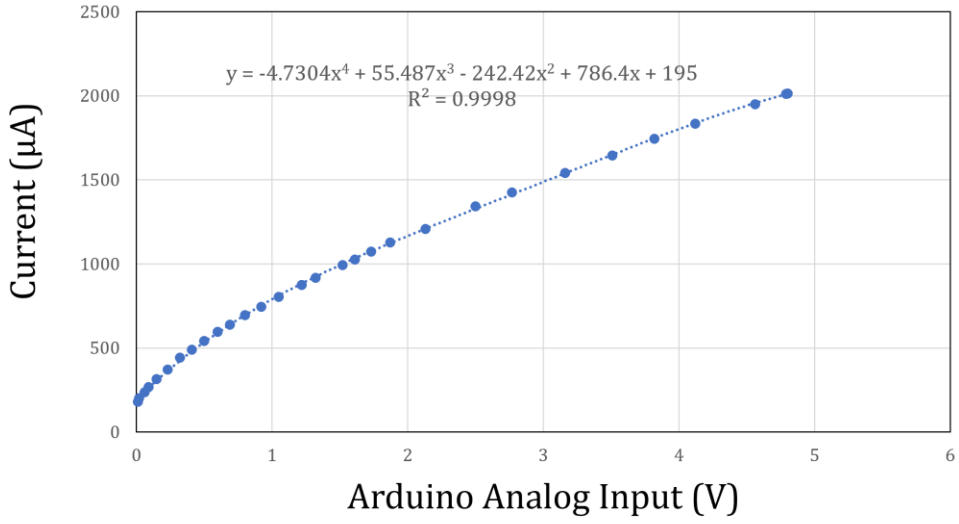

Figure 23. Calibration data for current measurement device. The current going through the LED as measured by a multimeter is plotted against the Arduino analog input.

The Arduino Uno used in the voltage and current measurement device runs the code given in Appendix A. This code allows the Arduino to be queried over USB and returns the raw and converted values for both the current and voltage measurements using the resistor values for the voltage and the calibration fit for the current.

3.4. Monitoring and Control System

3.4.1. Radiation Measurement and Safety

Because plasmas produce high energy X-rays and neutrons, it would not be safe for the operators to be near the fusor without precautions. When operating the fusor at high voltages with air, X-rays are predicted so a Ludlum Model 3 X-ray survey meter connected to a Ludlum Model 44-7 detector was directed at the hot cathode ion gauge connected to port 9, since this was the most X-ray penetrable point of the fusor. A small, wired webcam was attached to a ring stand and pointed at the survey meter, so the meter could be monitored throughout fusor operation. Another ring stand held an Android S21 Phone in front of the viewport on port 5. The phone ran the DroidCam app, allowing for the interior of the chamber to be seen at all times by connecting via WiFi. In the future, when the Fusor is eventually tested with deuterium, neutrons will be produced which will penetrate the steel

chamber. These neutrons would be monitored with a Ludlum Model 12-4 Neutron dose survey meter set outside of the chamber.

As a precaution taken to ensure the safety of operators, the fusor is designed to be operated remotely. Figure 24 is a diagram of the remote control system.

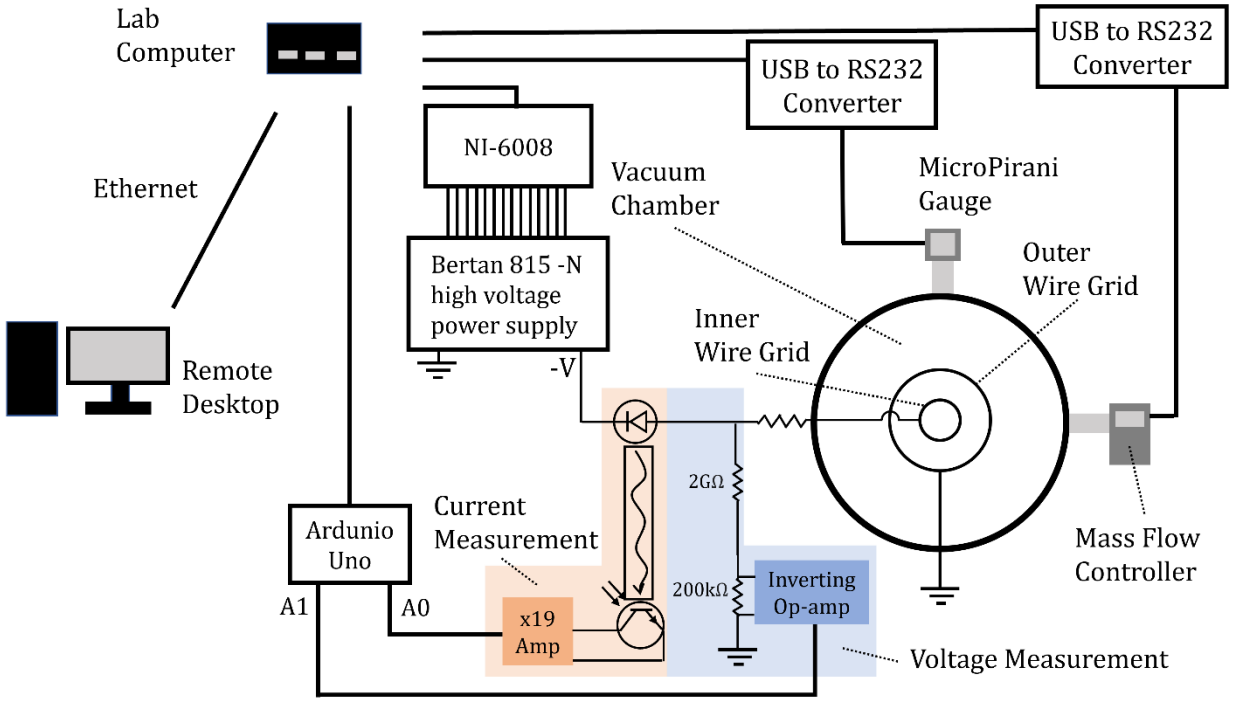

Figure 24. Block diagram of control system. A computer in a separate room connects remotely via ethernet to the computer near the fusor which uses a USB protocol to communicate with all peripherals. The mass flow controller and the MicroPirani pressure gauge require RS-232 communication, so a USB to R232 adapter was used. The computer communicates with the HV tunnel directly via USB, while it controls the power supply indirectly, by communicating with an NI-6008 to control digital and analog outputs which are connected to the power supply.

For the fusor to function remotely, the mass flow controller, the microPirani pressure gauge, the HV power supply, and the current and voltage measurement device must be accessed through a lab computer from a remote desktop. Both the mass flow controller and the microPirani gauge communicate using RS-232 serial interface, so adapters are used so they can be controlled using standard USB. While the current and voltage measurement device works with USB, the high voltage power supply does not, so the power supply is controlled

using a National Instruments USB 6008 data acquisition device which communicates over USB with the lab computer. The high voltage power supply has a variety of pins for which analog voltages from the NI-6008 are either applied to or read. These voltages control the power supply. The connections between the NI 6008 and the power supply are shown in Figure 25. The VOUT Program Monitor, which indicates the measured voltage from the power supply, was consistently similar to the set point written to the power supply using the VOUT Program Input pins, indicating it was working. The VOUT Program Output, which should indicate the set point, was constant for all voltage set points and measured voltages, indicating it was not working. Similarly, all of the IOUT pins were constant regardless of the current measured from the cathode, indicating they were also broken. The Enable Input of the HV power supply must be brought to ground for the High Voltage to be enabled. It is attached to the ground pin through a plug housing, so the other side of the plug acts as a digital key, physically enabling the power supply. The Remote Output must be brought to ground for the HV power supply to be controlled through the analog signals, so it is connected to one of the digital outputs of the NI 6008, allowing for remote enabling.

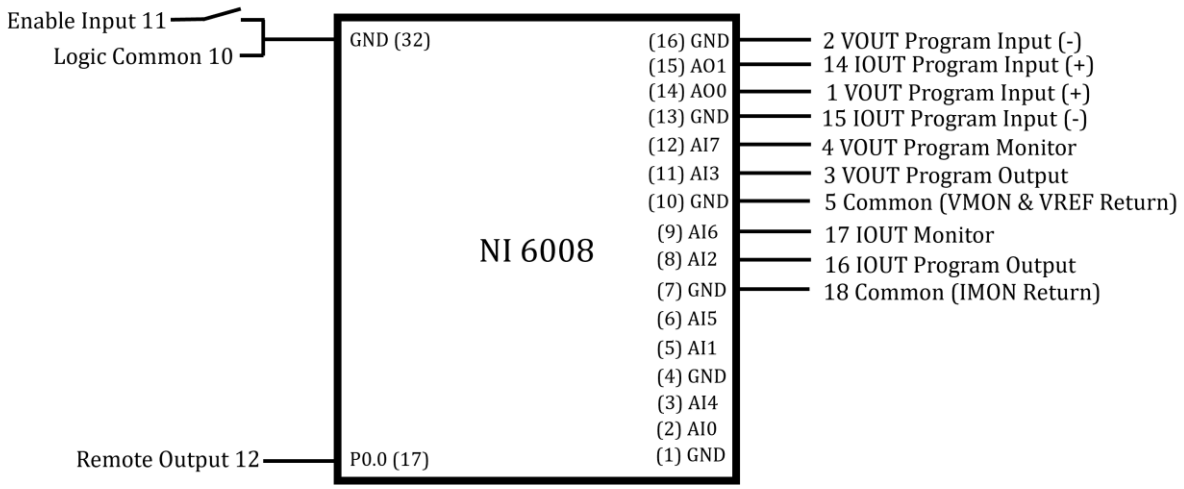

Figure 25. NI 6008 to HV Power Supply Connections Diagram. The NI 6008 is controlled over USB and connects to the various pins on the power supply as shown.

3.4.2. Manual Control

The python code in Appendix B, when run on the lab computer and accessed through the remoted desktop, displays the digital control panel in Figure 26, allowing for monitoring and control of the various instrumentation. For the HV power supply to operate, not only must the physical key be inserted to connect pin 11 of the HV power supply to ground as shown in Figure 25, but the digital signal must also be written to pin 12 which is accomplished when the "Enable/Disable" button is pressed on the lower left of the control panel, digitally enabling the power supply. The control panel displays the pressure of the chamber, the mass-flow rate entering the chamber, the voltage of the power supply, and the current going to the power supply from the cathode caused by ions hitting the -HV electrode. The voltage and current are readout both by the power supply and the current and voltage measurement device. Pressing the "Log" button on the bottom right of the control panel saves all of the measurements and set points as well as the current time to an Excel spreadsheet.

To operate the fusor manually, the pressure in the chamber is brought to approximately 4.7×10^{-3} Torr, corresponding to a mass flow rate of 3.5 sccm for air. The power supply voltage is then raised until plasma is formed, typically around 3.5 kV in air at this pressure. The formation of the plasma can be observed from the characteristic purple glow within the chamber through the webcam or when the current dramatically increases. Because fusion occurs at higher energies, the goal is to bring the voltage all the way to the full 30 kV supplied by the power supply without losing the plasma. When the voltage is raised, the current from the cathode goes up as well. Because the power supply is only capable of providing 3.3 mA or less, the pressure within the chamber must be reduced such that the plasma is still present, but the current is not too high. This means that when manually controlling the fusor, after the initial plasma is formed, the pressure must be reduced then the voltage quickly raised. This iterative process of incrementally lowering the pressure then adjusting the voltage is difficult and time consuming since the plasma is not a steady state, where a particular voltage and pressure always correspond to a certain current. Often, rather, the current can depend on the previous state of the system and the plasma is lost if the pressure or voltage is adjusted too much. For this reason, a system was designed to complete this process automatically.

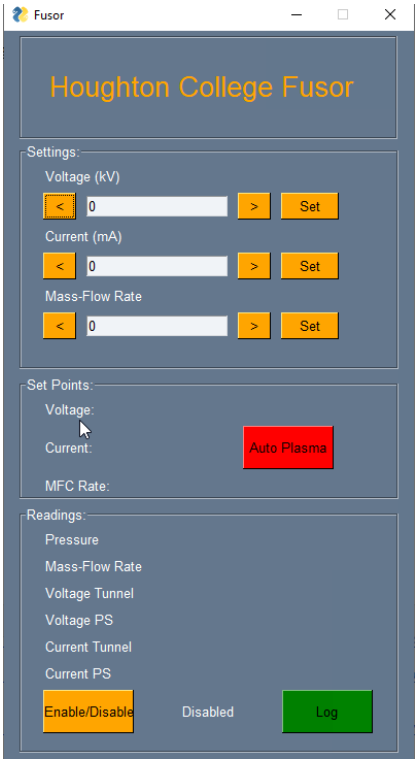

Figure 26. Screenshot of control panel. The limiting voltage and current of the power supply, as well as the mass flow rate, can be adjusted by either typing a number into the text box, or incremented with the arrows then clicking the "Set" button. The present set points are monitored in the "Set Points" section. The measured pressure, mass flow rate, and the voltage of the power supply as well as the current from the cathode are all displayed in the "Readings" section. All values at a particular instant can be appended to an excel spreadsheet along with the current time by pressing the green "Log" button. The Red Auto plasma button sets the mode to automatic.

3.4.3. Automatic Control System

While manually controlling the device consists of setting the pressure and then adjusting the voltage incrementally, the automatic control system does the opposite. The voltage is set, then the pressure is adjusted. A basic flow diagram of the system can be observed in Figure 27. First, the mass-flow controller is set to a particular flow rate and the power supply is set to a certain voltage. The current is then measured and compared with a target current (between 1.5 mA and 2.5 mA). The difference between the target and measured current at a particular time step, t, is the error, $e(t)$. The error is then passed into a proportional-integral-derivative (PID) function. This function consists of three terms which are then summed together to indicate the necessary adjustment to the mass flow controller.

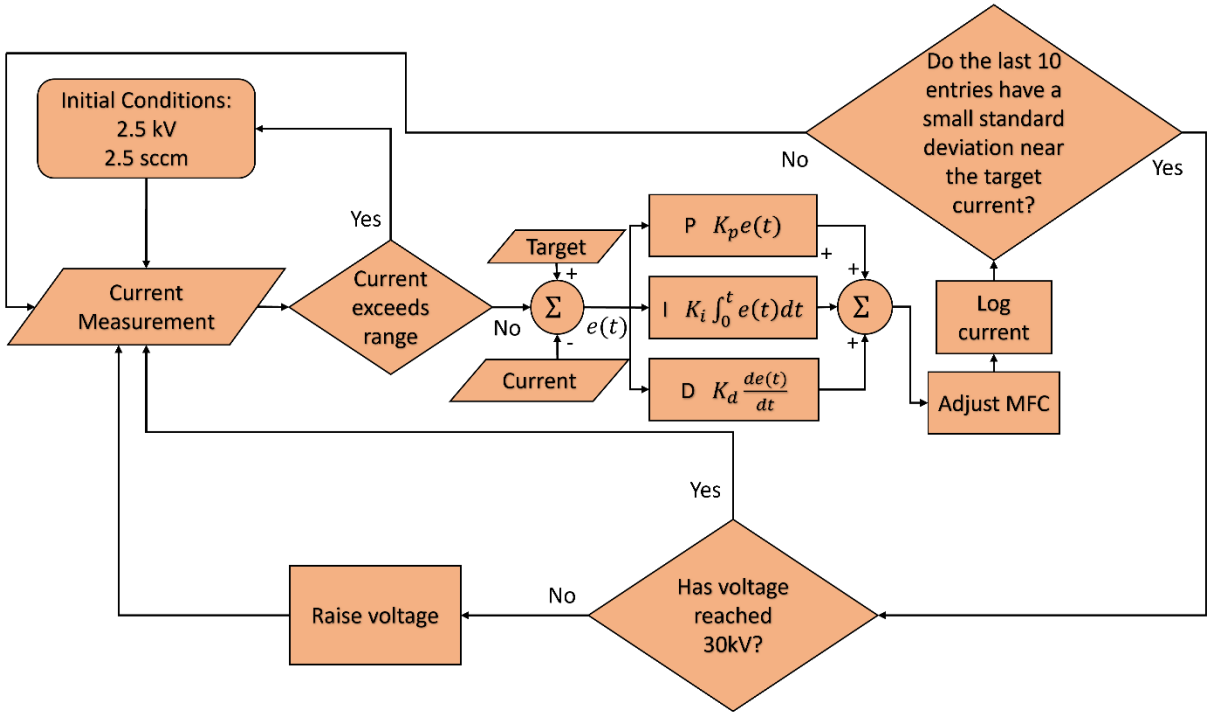

Figure 27. Flow diagram of automated control system. First, the voltage and flow rate are set to the initial conditions and the current measurement is compared to the target current. The resulting error is passed through a PID loop where the output is the adjustment for the mass flow controller. If the current is stable, the voltage is raised. This process is repeated until the voltage reaches 30 kV unless the current exceeds a maximum value or is lost entirely in which case the entire system starts over at the initial conditions.

The first term, known as the proportional term, P, is

$$P = K_p e(t), \tag{60}$$

where K_p is a constant and $e(t)$ is the error. The proportional term is responsible for producing significant changes in the controller for large errors. The second term, the integral term, I, is

$$I = K_i \int_0^t e(t)dt, \tag{61}$$

where K_i is a constant. The integral term serves to make small adjustments over time if previous adjustments were routinely insufficient. Finally, the last term, the derivative term, D, is given by

$$D = K_d \frac{de(t)}{dt}, \tag{62}$$

where K_d is a constant. The derivative term helps to prevent the system from overshooting the target by slowing down the changes as the target and measured value get closer together.

The sum of the P, I, and D terms is the amount the mass flow rate is adjusted. The mass flow controller is continually adjusted in this way, creating a stable plasma. At each time step, the current measurement is added to a log array. The last ten entries of the log are compared, and if the standard deviation is within 300 μA and the average is within 300 μA of the target current, the voltage is raised by 0.1 kV assuming the maximum of 30 kV has not been reached. The 300 μA value, along with the values of K_p, K_i and K_d, were determined arbitrarily and adjusted during experiments. Using this algorithm, at the press of a button, the plasma should form, and the pressure adjusted such that the voltage rises to 30 kV automatically while maintaining a stable plasma.

Chapter 4

RESULTS AND DATA ANALYSIS

4.1. Overview

Two experiments were conducted with the fusor. The first consisted of manually adjusting the voltage and pressure with air to create the necessary conditions for a plasma to form. The second experiment tested the automatic control system.

4.2. Manual Control Experiment and Results

For the manual control test, the mass flow controller was set to 3.5 sccm for air. The voltage was then increased by 0.2 kV starting at 2 kV until a plasma formed at 2.5 kV. This was observed from the webcam looking into the viewport as well as observing the current measurement on the display of the control panel which jumped from zero to 270 μA. Once the plasma formed, the pressure was lowered slightly by lowering the mass flow rate in increments of 0.2 sccm. The voltage was then raised quickly to prevent the plasma from being lost. This process was repeated until the voltage reached approximately 8 kV. Due to the dynamic nature of the plasma, the pressure and voltage had to be adjusted regularly to prevent the current from exceeding the 3.3 mA limit of the power supply or losing the plasma. Once the plasma was lost, the entire process had to be restarted, beginning with a voltage of 2 kV and a mass flow setting of 3.5 sccm. For this reason, the plasma was never sustained above 8 kV.

Since the pressure and voltage of the fusor are the controlled values that affect the current, these properties are plotted in Figure 28 for all points for which data were in the manual experiment, and a plasma existed. For the plasma to exist, the current must be greater than zero, so points with no current were not plotted. Notice how the pressure starts high and the voltage starts low. These values are then adjusted such that the current does not get too large, or the plasma disappears entirely.

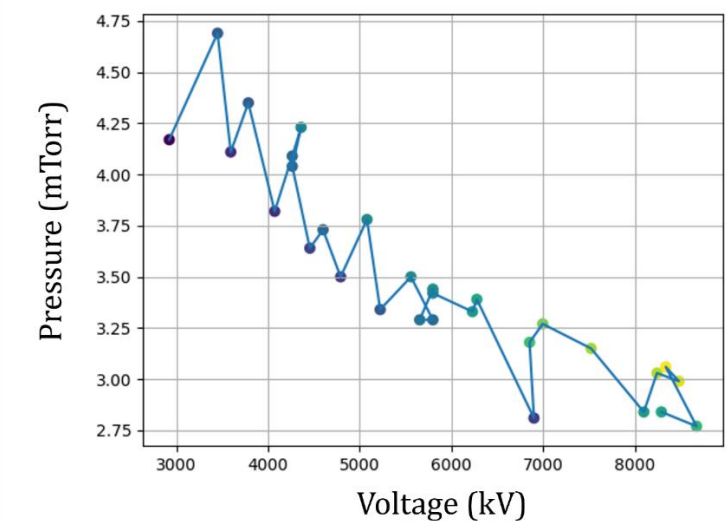

Figure 28. Chamber pressure vs. cathode voltage through time. The lines indicate the order in which the states existed. Current is indicated by the color of the points. Lighter points indicate a larger current. Notice the light yellow points on the right. This is where the current became too large for the power supply to keep up with, so the voltage was dropped to 2 kV and the plasma lost.

Figure 29 shows an image of the plasma from the manual test. Notice how the plasma seems to have an increased density in certain areas outside of the inner spherical cathode. This is characteristic of the "star mode" operation of a Farnsworth-Hirsch fusor.

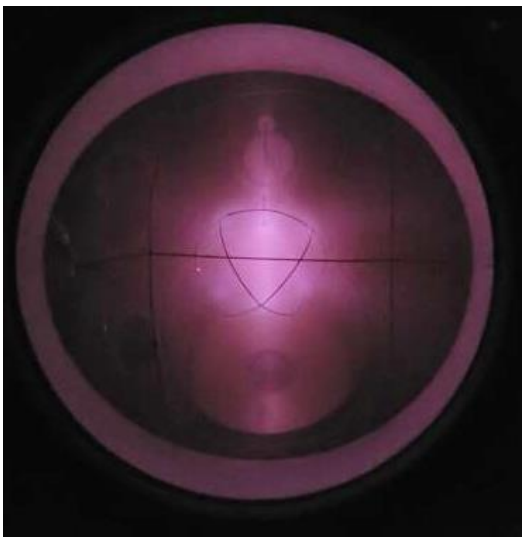

Figure 29. "Star mode" operation of fusor with air. The photograph was taken outside of a viewport by a Samsung S21 being used as a webcam.

4.3. Automatic Control Experiment and Results

The second experiment consisted of testing the automatic control of the pressure and voltage. The target current was initially set to 2.5 mA. Once the "Auto Plasma" button was pressed, the system was able to form a plasma, stabilize it, and increment the voltage to approximately 7 kV while maintaining a stable plasma. From this point forward though, as the autonomous system attempted to raise the set point of the power supply, the actual voltage did not change. As can be seen in Figure 30, from a set point starting at 5 kV until 6 kV the setpoint of the power supply is proportional to that measured with the voltage measurement device. From a set point of 6 kV on though, the measured voltage fails to increase and begins to fluctuate significantly. This indicates the power supply was unable to keep up with the target current of 2.5 mA.

As an attempt to remedy this issue, the target current was lowered to 2 mA. At this current though, the PID controller was unable to respond effectively enough to the changes in current to prevent loss of plasma. The PID weights were adjusted along with the standard deviation value, but in every configuration attempted the plasma was lost after the HV power supply reached just a few kV.

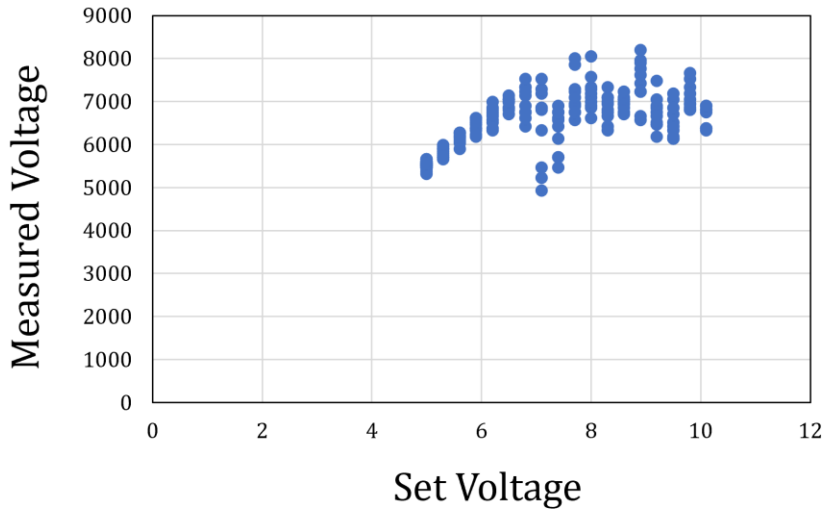

Figure 30. Set voltage vs. measured voltage. Notice the plot is linear when the set voltage is less than 6kV. After 6kV, the measured voltage does not seem to be correlated with the set point.

Chapter 5

CONCLUSIONS AND NEXT STEPS

5.1. Conclusions

The remote operating system of the Houghton University Farnsworth-Hirsch fusor has been redesigned, including replacing the TS4 Port servers with a National Instruments 6008 to control the HV power supply and rewriting the control system code in python. Furthermore, a device has been invented to measure both the current from the cathode by using the light from an LED and the voltage between the output terminal of the power supply and ground using a voltage divider. A first attempt at a fully automatic control system for forming and stabilizing a plasma as the voltage is raised has been created using a PID controller. The fusor was operated manually, but a power supply voltage of 8 kV was the maximum reached before the plasma was lost due to difficulties in adjusting the pressure and voltage quickly enough. The automatic control system was able to create and maintain a plasma while raising the voltage up to 7 kV when the target current was set to 2.5 mA, but the power supply was unable to keep up with this current, so the voltage was never raised beyond 7 kV. When the target current was lowered to 2 mA the control system was unable to respond effectively enough to maintain the plasma.

5.2. Future Work

A first step toward making the fusor operational would be to fix the automated control system. One solution might be to adjust the baud rate of the Arduino, allowing for an increased number of iterations per time in the automated control loop. This could resolve the issue of the PID control not being able to maintain the plasma, since it is unable to adjust the pressure adequately enough for a lower target current. This problem may also stem from the fact that a change in the mass flow controller takes time before a change in the chamber pressure is observed. A potential way to resolve this would be to alter the automatic control such that small changes in voltages are allowed in addition to the smaller changes in pressure. This would resolve the issue as the response time for a voltage change to the cathode is much shorter than the pressure change from an altered mass flow rate. Another

possibility is that the PID parameters need to be tuned, which would require further testing and a methodical approach to adjusting the parameters.

Once the issues with the automated control system have been resolved, or the manual control has been successfully completed using the new control system so that the full 30 kV potential of the power supply can be used, hydrogen will be introduced into the chamber instead of air. The previously completed updates to the feed through can then be tested to determine if they are sufficient to prevent sparking in the chamber. Finally, deuterium will be used as the gas in the chamber so that D-D fusion can be observed. Notice in Figure 31, the cross section for a D-D reaction when the particles have an incident energy of 30 keV is significant enough that a noticeable number of reactions will be produced. The neutrons that result from these reactions will be measured using a neutron dose survey meter and X-rays produced will be monitored by a survey meter.

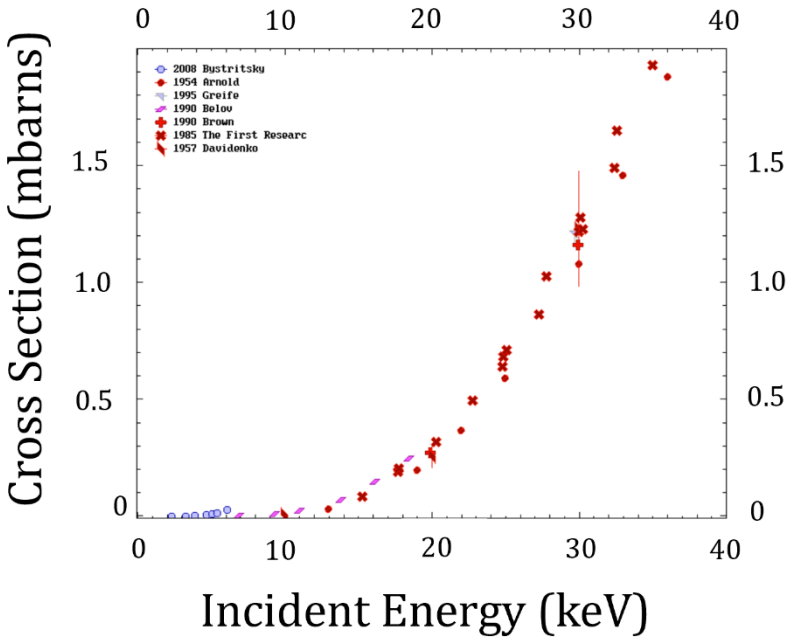

Figure 31. Cross section as function of incident energy for a D-D Reaction. Notice that there is a significant cross section (approximately 1.3 mbarns) at an incident energy of 30 keV. Plot taken from Ref [20].

Appendix A

ARDUINO CODE FOR VOLTAGE AND CURRENT MEASUREMENT DEVICE

```
const int currentPin = A0;
const int voltagePin = A1;

double currentReading, voltageReading;
double rawCurrentVoltage, rawVoltage;
double calculatedCurrent, calculatedVoltage;

//For current calculation, taken from calibration data
const double a_4 = -4.7304;
const double a_3 = 55.487;
const double a_2 = -242.42;
const double a_1 = 786.4;
const double a_0 = 195;

//For voltage calculation
const double R2_R1 = 9804;//calculated as voltage divider - 2GOhms/204.1kohms


void setup() {
  Serial.begin(9600);
  pinMode(currentPin, INPUT);
  pinMode(voltagePin, INPUT);
}

void loop() {
  // put your main code here, to run repeatedly:
  currentReading = analogRead(currentPin);
  voltageReading = analogRead(voltagePin);

  //1023 is max analog reading of Arduino corresponding to 5V max
  rawCurrentVoltage = (currentReading/1023)*5;
  rawVoltage = (voltageReading/1023)*5;

  //current reading based on voltage reading from calibration data
  calculatedCurrent = a_4*pow(rawCurrentVoltage, 4) +
    a_3*pow(rawCurrentVoltage, 3) +
    a_2*pow(rawCurrentVoltage, 2) +
    a_1*pow(rawCurrentVoltage, 1) + a_0;

  calculatedVoltage = R2_R1*rawVoltage;

  Serial.print("R");
  Serial.print(rawCurrentVoltage);
  Serial.print("C");
  Serial.print(calculatedCurrent);
  Serial.print("r");
  Serial.print(rawVoltage);
  Serial.print("c");
  Serial.println(calculatedVoltage);
```

```
  //check for query
  if(Serial.available()){
        input = Serial.read();
        if(input == "R"){
          Serial.print("M");
          Serial.println(getRawCurrentVoltage());
        }
  }

}

double getRawCurrentVoltage(){
  currentReading = analogRead(currentPin);
  rawCurrentVoltage = (currentReading/1023)*5;

}
```

Appendix B

PYTHON CONTROL CODE

```
import pandas as pd #required for logging
import openpyxl
from datetime import datetime #required for keeping track of time
import PySimpleGUI as sg #required for GUI
from matplotlib.backends.backend_tkagg import FigureCanvasTkAgg,
FigureCanvasAgg  #required for GUI

import serial #for Arduino
import nidaqmx #for NI6008 (which controls HV power supply)
from nidaqmx.constants import (TerminalConfiguration)
import pyvisa #for MFC and pressure gauge

import time
import numpy as np

#log is a list that data is appended to.
log = []

#RSE analog inputs
HV_current_program_out = "Dev1/ai2" #pin ai2
HV_current_mon_out = "Dev1/ai6" #pin ai6

HV_voltage_program_out = "Dev1/ai3" #pin ai2
HV_voltage_mon_out = "Dev1/ai7" #pin ai6

#analog outputs
HV_voltage_set_pin = "Dev1/ao0"
HV_current_set_pin = "Dev1/ao1"


class pid_controller():
    def __init__(self):
        self.max_current = 2500
        self.min_current = 200 #effectively 0
        self.max_voltage = 29.9
        self.max_flow_rate = 5
        self.default_flow_rate = 2.5
        self.default_voltage = 7
        self.voltage_increment = 0.3
```

```
        self.target = 1500
        self.max_std = 300 #determines how close last 10 measurements have to
be to target and how spread out they can be for v to be increased

        self.kp = 0.00003
        self.ki = 0.00002
        self.kd = 0.00003

        self.acc = 0
        self.last_error = 0
        self.last_time = 0

        self.current_log = []
        self.starting = True

    def pid(self, state):
        error = self.target - state
        proportional = error*self.kp
        integral = self.acc + self.ki*error

        current_time = time.time()
        deltaT = current_time - self.last_time
        self.lastTime = current_time

        derivative = self.kd*(error - self.last_error)/deltaT
        self.last_error = error

        adjustment = proportional + integral + derivative

        return adjustment

    def get_values(self, voltage_state, mass_flow_state, current_state):
        #make sure current does not get too high, if it is set pressure and
voltage to default values
        if current_state > self.max_current or ((current_state <
self.min_current) and self.starting==False):
            print(f'Current exceeded range {current_state}')
            flow_rate = self.default_flow_rate
            voltage = self.default_voltage
            self.starting=True
            return voltage, flow_rate

        #otherwise
        if (current_state > self.min_current + self.max_std):
```

```
            self.starting = False

        self.current_log.append(current_state)#note the current

        #if there have been at least 10 measurements of current since last
changing the voltage
        if (len(self.current_log) >= 10):
            self.current_log = self.current_log[-10:]
            #calculate standard deviation and mean of last 10 current entries
            std = np.std(self.current_log)
            mean = np.mean(self.current_log)

            #if the current is not fluctuating too much and they are close to
what they should be
            if std < self.max_std and np.abs(mean-self.target) <
self.max_std:
                #increase voltage
                prop_v = voltage_state + self.voltage_increment
                if (prop_v < self.max_voltage):
                    voltage = prop_v
                else:
                    voltage = voltage_max

                self.current_log = []
            else:
                voltage = voltage_state
        else:
            voltage = voltage_state

        delta_mf = self.pid(current_state)

        prop_fr = mass_flow_state + delta_mf
        if prop_fr < self.max_flow_rate:
            flow_rate = prop_fr
        else:
            flow_rate = self.max_flow_rate

        return voltage, flow_rate

    def get_default(self):
        return self.default_voltage, self.default_flow_rate



#initialize all devices
```

```
def initialize_devices():
    # configure the devices
    print("\033[1mHoughton College Fusor \033[0m \n")
    print("(c) 2023 Micah Condie")
    print("Initializing:\n")
    print("setting up pressure gauge...")

    rm = pyvisa.ResourceManager()
    #print(rm.list_resources()) #for debugging

    #set up pressure gauge
    print("Setting up Pressure Gauge")
    pg = rm.open_resource('ASRL8::INSTR')
    pg.read_termination = ';'

    #set up MFC
    print("Setting up Mass-Flow Controller")
    mfc = rm.open_resource('ASRL28::INSTR')
    mfc.read_termination = '\r'
    mfc.write_termination = '\r'

    #set up Arduino
    print("Setting up Arduino")
    arduino = serial.Serial(port='COM30', baudrate=9600, timeout=1)

    return pg, mfc, arduino



#Define how display will look
col1 = sg.Column([
    # title
    [sg.Frame('',[
        [sg.Text(' ')],
        [sg.Text('  Houghton College Fusor', size=(20, 1), font=("Helvetica",
20),text_color='orange')]
        ], size=(367,100),  pad=(5,0))
    ],
    [sg.Frame('Settings:',[
                            [sg.Text(),
                                 sg.Column([
                                    [sg.Text('Voltage (kV)')],
                                    [sg.Button('<', size=(3, 1),
button_color=('black', 'orange'), key='VDown'),
```

```
                                    sg.Input(key='-VOLTAGE-SETTING-',
default_text="0", size=(19,1)),
                                    sg.Button('>', size=(3, 1),
button_color=('black', 'orange'), key='VUp'),
                                    sg.Button('Set', size=(6, 1),
button_color=('black', 'orange'), key='VSet')
                                    ],
                                   [sg.Text('Current (mA)')],
                                   [sg.Button('<', size=(3, 1),
button_color=('black', 'orange'), key='IDown'),
                                    sg.Input(key='-CURRENT-SETTING-',
default_text="0", size=(19,1)),
                                    sg.Button('>', size=(3, 1),
button_color=('black', 'orange'), key='IUp'),
                                    sg.Button('Set', size=(6, 1),
button_color=('black', 'orange'), key='ISet')
                                    ],

                                   [sg.Text('Mass-Flow Rate')],
                                   [sg.Button('<', size=(3, 1),
button_color=('black', 'orange'), key='MDown'),
                                    sg.Input(key='-MASS-FLOW-SETTING-',
default_text="0", size=(19,1)),
                                    sg.Button('>', size=(3, 1),
button_color=('black', 'orange'), key='MUp'),
                                    sg.Button('Set', size=(6, 1),
button_color=('black', 'orange'), key='MSet')
                                    ]
                                   ], size=(350,200), pad=(0,0))
                           ]
                       ]
             )
      ],

    [sg.Frame('Set Points:', [
                            [sg.Text(),
                                sg.Column([
                                   [sg.Text('Voltage:'),
sg.Text(size=(15,1), key='-VOLTAGE-SET-POINT-CONVERTED-')],
#sg.Text(size=(15,1), key='-VOLTAGE-SET-POINT-')
                                    [sg.Text('Current:'),
sg.Text(size=(15,1), key='-CURRENT-SET-POINT-CONVERTED-'), sg.Button('Auto
Plasma', size=(10, 2), button_color=('black', 'Red'), key='auto')], #
sg.Text(size=(15,1), key='-CURRENT-SET-POINT-'),
```

```
                                    [sg.Text('MFC Rate:'),
sg.Text(size=(15,1), key='-MASS-FLOW-SET-POINT-')],
                                    ], size=(350,100), pad=(0,0))
                            ]
                        ]
                )
     ],

    [sg.Frame('Readings:', [
                             [sg.Text(),
                                 sg.Column([
                                    [sg.Text('Pressure'),
sg.Text(size=(15,1), key='-PRESSURE-READ-')],
                                    [sg.Text('Mass-Flow Rate'),
sg.Text(size=(15,1), key='-MASS-FLOW-READ-')],
                                    [sg.Text('Voltage Tunnel'),
sg.Text(size=(15,1), key='-VOLTAGE-TUNNEL-READ-'), sg.Text(size=(15,1),
key='-VOLTAGE-TUNNEL-READ-CONVERTED-')],
                                    [sg.Text('Voltage PS'),
sg.Text(size=(15,1), key='-VOLTAGE-PS-READ-'), sg.Text(size=(15,1), key='-
VOLTAGE-PS-READ-CONVERTED-')],
                                    [sg.Text('Current Tunnel'),
sg.Text(size=(15,1), key='-CURRENT-TUNNEL-READ-'), sg.Text(size=(15,1),
key='-CURRENT-TUNNEL-READ-CONVERTED-')],
                                    [sg.Text('Current PS'),
sg.Text(size=(15,1), key='-CURRENT-PS-READ-'), sg.Text(size=(15,1), key='-
CURRENT-PS-READ-CONVERTED-')],
                                    [sg.Button('Enable/Disable', size=(10,
2), button_color=('black', 'orange'), key='enable_disable'),
sg.Text('Disabled', size=(15,1), key='-ENABLED-'), sg.Button('Log', size=(10,
2), button_color=('black', 'green'), key='log')]
                                    ], size=(350,220), pad=(0,0))
                            ]
                        ]
                )
     ],], pad=(0,0))

layout = [[col1]]


def save_log():
    now = datetime.now()
    file_name = "Fusor_" + now.strftime("%m:%d:%H:%M").replace(":", "_" )
    col_names = ['Time',
                 'Set Voltage',
```

```
                    #'V monitor out raw',
                    'V monitor out converted',
                    'V program out raw',
                    'V program out converted',
                    'HV Tunnel Measured Voltage Raw',
                    'HV Tunnel Measured Voltage Converted',
                    'Set Current',
                    #'I Monitor Raw',
                    'I Monitor Converted',
                    'I Program Out Raw',
                    'I Program Out Converted',
                    'HV Tunnel Measured Current Raw',
                    'HV Tunnel Measured Current Converted',
                    'Set Mass-Flow Rate',
                    'Set Point Mass-Flow Rate from MFC',
                    'Mass-Flow Rate',
                    'Pressure',
                    'Pressure Converted']
    df2 = pd.DataFrame(log, index=[x for x in range(1, len(log)+1)],
columns=col_names)
    df2.to_excel(f'log\{file_name}.xlsx')

#logs what is on window as well as the values in the text boxes
def log_values(values, window):
    now = datetime.now()
    current_time = now.strftime("%H:%M:%S")
    status_values = [current_time,
                    float(values['-VOLTAGE-SETTING-']),
                    #float(window['-VOLTAGE-SET-POINT-'].get()),
                    float(window['-VOLTAGE-SET-POINT-CONVERTED-'].get()),
                    float(window['-VOLTAGE-PS-READ-'].get()),
                    float(window['-VOLTAGE-PS-READ-CONVERTED-'].get()),
                    float(window['-VOLTAGE-TUNNEL-READ-'].get()),
                    float(window['-VOLTAGE-TUNNEL-READ-CONVERTED-'].get()),
                    float(window['-CURRENT-SETTING-'].get()),
                    #float(window['-CURRENT-SET-POINT-'].get()),
                    float(window['-CURRENT-SET-POINT-CONVERTED-'].get()),
                    float(window['-CURRENT-PS-READ-'].get()),
                    float(window['-CURRENT-PS-READ-CONVERTED-'].get()),
                    float(window['-CURRENT-TUNNEL-READ-'].get()),
                    float(window['-CURRENT-TUNNEL-READ-CONVERTED-'].get()),
                    float(values['-MASS-FLOW-SETTING-']),
                    float(window['-MASS-FLOW-SET-POINT-'].get()),
                    float(window['-MASS-FLOW-READ-'].get()),
                    "=" + window['-PRESSURE-READ-'].get(),
```

```
                0]
    log.append(status_values)


def main():

    #PS requires being both physically enabled and digitally (signal brought
to low). Enabled var controls the latter.
    enabled = False

    #not staring in auto mode
    automatic = False
    #ititialize devices
    pg, mfc, arduino = initialize_devices()

    # create window
    window = sg.Window('Fusor',  layout,
finalize=True,text_justification="center", element_justification="center")
    otto = pid_controller()
    #loop
    while True:

        #check if anything has happened, if it hasn't, update every second
anyway (timeout value)
        event, values = window.read(timeout=1000)

        #window closed
        if event == sg.WIN_CLOSED or event == 'exit':
            save_log()
            break


        #Buttons pressed that change the values of the text boxes (either up
or down).
        #Voltage (V), Current (I) or mass flow rate (M)
        if event == 'VDown':
             window['-VOLTAGE-SETTING-'].update(str(round((float(values['-
VOLTAGE-SETTING-']) - 0.5), 3)))

        elif event == 'VUp':
             window['-VOLTAGE-SETTING-'].update(str(round((float(values['-
VOLTAGE-SETTING-']) + 0.5), 3)))

        elif event == 'IDown':
```

```
            window['-CURRENT-SETTING-'].update(str(round((float(values['-
CURRENT-SETTING-']) - 0.1), 3)))

        elif event == 'IUp':
            window['-CURRENT-SETTING-'].update(str(round((float(values['-
CURRENT-SETTING-']) + 0.1), 3 )))

        elif event == 'MDown':
            window['-MASS-FLOW-SETTING-'].update(str(float(values['-MASS-
FLOW-SETTING-']) - 0.1))

        elif event == 'MUp':
            window['-MASS-FLOW-SETTING-'].update(str(float(values['-MASS-
FLOW-SETTING-']) + 0.1))

        #Log button pressed
        elif event == 'log':
            log_values(values, window)

        #Buttons pressed that affect the output of the instruments
        #set voltage
        elif event == 'VSet':
            voltage_setting = float(values['-VOLTAGE-SETTING-'])
            voltage_out = voltage_setting/6#converts the desired voltage (kV)
to the output of NI6008 (V). 0-30kV -->0-5V
            with nidaqmx.Task() as t:
                t.ao_channels.add_ao_voltage_chan(HV_voltage_set_pin,
min_val=0.0,max_val=5.0)
                t.write(voltage_out)
                t.stop()
        #set current
        elif event == 'ISet':
            current_setting = float(values['-CURRENT-SETTING-'])
            current_out = current_setting*(5/3.3)#converts the desired
current (mA) to the output of NI6008 (V). 0-3.3mA -->0-5V
            with nidaqmx.Task() as t:
                t.ao_channels.add_ao_voltage_chan(HV_current_set_pin,
min_val=0.0,max_val=5.0)
                t.write(current_out)
                t.stop()

        #set mass flow rate
        elif event == 'MSet':
            val = f"AS{values['-MASS-FLOW-SETTING-']}"
            mfc.query(val)
```

```
        #enable or disable the power supply
        elif event == 'enable_disable':
            enabled = not enabled
            print(enabled)
            if(enabled):
                current_status = window['-ENABLED-'].update("Enabled")
            else:
                current_status = window['-ENABLED-'].update("Disabled")

            task = nidaqmx.Task()
            task.do_channels.add_do_chan("Dev1/port0/line0")
            task.start()
            task.write(not enabled)#low enables, high disables
            task.stop
            task.close()

        #turn auto on
        elif event == 'auto':
            automatic = not automatic
            if automatic:
                control_voltage, control_flow_rate = otto.get_default()
                voltage_out = control_voltage/6#converts the desired voltage
(kV) to the output of NI6008 (V). 0-30kV -->0-5V
                with nidaqmx.Task() as t:
                    t.ao_channels.add_ao_voltage_chan(HV_voltage_set_pin,
min_val=0.0,max_val=5.0)
                    t.write(voltage_out)
                    t.stop()
                window['-VOLTAGE-SETTING-'].update(str(round(control_voltage,
3)))

                window['-MASS-FLOW-SETTING-'].update(str(control_flow_rate))
                val = f"AS{control_flow_rate}"
                mfc.query(val)




        #Read all instruments and update screen regardless of if anything was
pressed

        #read NI6008
        with nidaqmx.Task() as task:
```

```
            task.ai_channels.add_ai_voltage_chan(HV_current_program_out,
terminal_config=TerminalConfiguration.RSE, min_val=-5, max_val=5)
            task.ai_channels.add_ai_voltage_chan(HV_current_mon_out,
terminal_config=TerminalConfiguration.RSE, min_val=-5, max_val=5)
            task.ai_channels.add_ai_voltage_chan(HV_voltage_program_out,
terminal_config=TerminalConfiguration.RSE, min_val=-5, max_val=5)
            task.ai_channels.add_ai_voltage_chan(HV_voltage_mon_out,
terminal_config=TerminalConfiguration.RSE, min_val=-5, max_val=5)

            analog_inputs = task.read()

        #Read HV Tunnle
        #raw current data
        arduino.write(b'c')
        line = arduino.readline().strip()
        line_str = str(line)
        raw_current_volt = float((line_str.split("'")[1])[1:])
        window['-CURRENT-TUNNEL-READ-'].update("%7.2f"%(raw_current_volt))

        #calculated current data
        arduino.write(b'C')
        line = arduino.readline().strip()
        line_str = str(line)
        calc_current = float((line_str.split("'")[1])[1:])
        window['-CURRENT-TUNNEL-READ-CONVERTED-
'].update("%7.2f"%(calc_current))

        #raw voltage data
        arduino.write(b'v')
        line = arduino.readline().strip()
        line_str = str(line)
        raw_volt = float((line_str.split("'")[1])[1:])
        window['-VOLTAGE-TUNNEL-READ-'].update("%7.2f"%(raw_volt))

        #calculated voltage data
        arduino.write(b'V')
        line = arduino.readline().strip()
        line_str = str(line)
        calc_volt = float((line_str.split("'")[1])[1:])
        window['-VOLTAGE-TUNNEL-READ-CONVERTED-'].update("%7.2f"%(calc_volt))

        #update window for NI6008
        voltage_set = float(analog_inputs[3])
        voltage_set_con = 6*voltage_set
        #window['-VOLTAGE-SET-POINT-'].update("%7.2f"%(voltage_set))
```

```
        window['-VOLTAGE-SET-POINT-CONVERTED-
'].update("%7.2f"%(voltage_set_con))

        current_set = float(analog_inputs[1])
        current_set_con = (3.3/5) *current_set
       # window['-CURRENT-SET-POINT-'].update("%7.2f"%(current_set))
        window['-CURRENT-SET-POINT-CONVERTED-
'].update("%7.2f"%(current_set_con))

        ps_voltage = float(analog_inputs[2])
        ps_voltage_con = 6*ps_voltage
        window['-VOLTAGE-PS-READ-'].update("%7.4f"%(ps_voltage))
        window['-VOLTAGE-PS-READ-CONVERTED-
'].update("%7.4f"%(ps_voltage_con))

        ps_current = float(analog_inputs[0])
        ps_current_con = (3.3/5)*ps_current
        window['-CURRENT-PS-READ-'].update("%7.2f"%(ps_current))
        window['-CURRENT-PS-READ-CONVERTED-
'].update("%7.2f"%(ps_current_con))

        #Read pressure gauge
        pressure_readout = pg.query("@253PR1?;FF")
        pressure = pressure_readout.split("K")[1]#.split[";"][0];

        #Read MFC
        mfc_values = mfc.query("A")
        mfc_arr = mfc_values.split(" ")
        mf_rate = mfc_arr[4]
        mfc_set_point = mfc_arr[5]


        window['-MASS-FLOW-SET-POINT-
'].update("%7.2f"%(float(mfc_set_point)))
        window['-PRESSURE-READ-'].update(pressure)
        window['-MASS-FLOW-READ-'].update("%7.2f"%(float(mf_rate)))


        if automatic:
            ###AUTO CONTROL###
            log_values(values,window)
            current_state = calc_current
            voltage_state = float(values['-VOLTAGE-SETTING-'])
            flow_rate_state = float(values['-MASS-FLOW-SETTING-'])
```

```
            control_voltage, control_flow_rate =
otto.get_values(voltage_state, flow_rate_state, current_state)
            window['-MASS-FLOW-SETTING-'].update(str(control_flow_rate))
            val = f"AS{control_flow_rate}"
            mfc.query(val)

            if (control_voltage != voltage_state):
                voltage_out = control_voltage/6#converts the desired voltage
(kV) to the output of NI6008 (V). 0-30kV -->0-5V
                with nidaqmx.Task() as t:
                    t.ao_channels.add_ao_voltage_chan(HV_voltage_set_pin,
min_val=0.0,max_val=5.0)
                    t.write(voltage_out)
                    t.stop()
                window['-VOLTAGE-SETTING-'].update(str(round(control_voltage,
3)))


if __name__ == '__main__':
    main()
```

R e f e r e n c e s

[1] A.S. Eddington, Science **52**, 233 (1920).

[2] S. Earnshaw, Transactions of the Cambridge Philosophical Society **7**, 97(1848).

[3]G.H. Miley and S. K. Murali, *Inertial Electrostatic Confinement Fusion: Fundamentals and Applications* (Springer, New York, 2014).

[4] N. Ghahramany, S. Gharaati, and M. Ghanaatian, Physics of Particles and Nuclei Letters **8**, 97 (2011).

[5] P.T. Farnsworth, U.S. Patent No. 3,258,402 (28 June 1966).

[6] T.J. Dolan, Plasma Physics and Controlled Fusion **36**, 1539 (1994).

[7] I. Hore-Lacy, *Nuclear Energy in the 21st Century: World Nuclear University Press* (Elsevier Science, Burlington, 2010).

[8] A.B. Zylstra *et. al.*, Physical Review E **106**, 2 (2022).

[9] J.D. Lawson, Proceedings of the Physical Society. Section B **70**, 6 (1957).

[10] R.W. Bussard, U.S. Patent No. 4,826,646 (2 May 1989).

[11] A. J. Wolf, Master Thesis, Eindhoven University of Technology, 1993.

[12] W.C. dElmore, J.L. Tuck, and K.M. Watson, Physics of Fluids **2**, 239 (1959).

[13] R.L. Hirsch, Journal of Applied Physics **38**, 4522 (1967).

[14] R.L. Hirsch, Physics of Fluids **11**, 2486 (1968).

[15] D.C. Barnes and R.A. Nebel, Physics of Plasmas **5**, 2498 (1998).

[16] G.H. Miley, *Life at the Center of the Energy Crisis: A Technologist's Search for a Black Swan* (World Scientific, Singapore, 2013).

[17] I. Love, Undergraduate Thesis, Houghton College, 2014.

[18] K. Craft, Undergraduate Thesis, Houghton College, 2016.

[19] J. D. Callen, Fundamentals of Plasma Physics, (University of Wisconsin-Madison), WWW Document, (http://homepages.cae.wisc.edu/~callen/chap5.pdf), 2003. (Unpublished)

[20] *National Nuclear Data Center NNDC*. Available at: http://www.nndc.bnl.gov/. (Accessed: 14 April 2023).